Qualitative Theory of Dynamical Systems (2023) 22:116
https://doi.org/10.1007/s12346-023-00821-z

Modelling the Dynamics in a Predator–Prey System with Allee Effects and Anti-predator Behavior

Tao Wen[1,2] · Yancong Xu[1] · Mu He[3] · Libin Rong[4]

Received: 1 March 2023 / Accepted: 1 June 2023 / Published online: 10 June 2023

Abstract

This paper studies a predator–prey model with strong and weak Allee effects and anti-predator behavior using a dynamical system approach. We perform a detailed bifurcation analysis including saddle-node bifurcation, Hopf bifurcation of codimension 3, cusp of codimension 3, cusp type Bogdanov–Takens bifurcation of codimension 3, and codimension-2 cusp of the limit cycle. The involvement of strong and weak Allee effects provides a new regime shift mechanism, which indicates the transition from a homoclinic cycle to a new heteroclinic cycle connecting two boundary equilibria induced by the Allee effect and the carrying capacity. The role of anti-predator behavior is fully uncovered by studying the interaction with the Allee effect. It is the first time that we find a codimension-2 cusp of infinitesimal limit cycle in the predator–prey system, which indicates the existence of a coexistence region of three limit cycles due to the weak Allee effect. Different from the scenario in the reference (Aguirre et al. in SIAM J Appl Math 69(5):1244–1262, 2009), it is a new generating mechanism of limit cycle bifurcating from one Hopf bifurcation point with two saddle-node bifurcation points on the limit cycle branch, and the double limit cycle curve originates from a codimension-2 degenerate Hopf bifurcation point and disappears at another one. The dynamics of the model with the Allee effect and anti-predator behavior are shown to be more complicated than those for other predator–prey systems. The biological interpretations of the bifurcation diagram and phase portrait are also provided.

✉ Yancong Xu
Yancongx@cjlu.edu.cn

1 Department of Mathematics, China Jiliang University, Hangzhou 310018, China

2 Department of Mathematics, Hangzhou Normal University, Hangzhou 311121, China

3 Department of Foundational Mathematics, Xi'an Jiaotong-Liverpool University, Suzhou 215028, China

4 Department of Mathematics, University of Florida, Gainesville, FL 32611, USA

Keywords Allee effect · Anti-predator · Codimension-3 Hopf bifurcation · Codimension-3 cusp type Bogdanov–Takens bifurcation · Codimension-2 cusp of limit cycle

1 Introduction

The local and global dynamics in predator–prey systems have been widely investigated by many researchers in order to uncover potential interactions. Based on the well-known Lotka–Volterra predator–prey model initiated by Lotka [1] and Volterra [2], many continuous and discrete models have been developed [3–18]. Zhu et al. [4] studied the following generalized Gause-type predator–prey system

$$\begin{aligned} \frac{dx}{dt} &= rx(\mathcal{K} - x) - p(x)y, \\ \frac{dy}{dt} &= y(-d + cp(x)), \end{aligned} \tag{1}$$

where x is the density of prey and y is the density of predator.

$$p(x) := \frac{mx}{ax^2 + bx + 1}, a > 0, b > -2\sqrt{a}, m > 0,$$

is a generalized Holling type IV response. Here r, $\mathcal{K}$, c and d denote the intrinsic growth rate of the prey population, the environmental carrying capacity of the prey, the constant of proportionality and the natural death rate of the predators, respectively. The parameters r, c, d and $\mathcal{K}$ are all positive. $p(x)$ is the functional response describing the change in the density of the prey attacked per unit of time per predator. It models the scenario where the prey can better defend or disguise themselves when their population becomes large enough, a phenomenon called group defense. The function $p(x)$ is positive when $x > 0$, and its derivative is positive when $x \in (0, \frac{1}{\sqrt{a}})$. It has the maximum at $x = \frac{1}{\sqrt{a}}$. Its derivative is negative when $x > \frac{1}{\sqrt{a}}$. The function goes to 0 as $x \to \infty$. This function can describe the effect of group defense (i.e. the prey can better defend themselves with a sufficiently large population) [10]. The related bifurcation analysis including saddle-node bifurcation, homoclinic bifurcation, and Bogdanov–Takens bifurcation of codimension 3 was investigated. The codimension-3 Bogdanov–Takens bifurcation acts as an organizing center for the system. The topological location of several kinds of bifurcation was studied in detail.

The Allee effect has been widely studied in predator–prey systems, which was proposed by Allee [19, 20]. It describes the relationship between population growth and population density. If the population density of a species is too sparse, its population will be reduced. According to the strong Allee effect, the sparse or dense population density will lead to negative growth, possibly causing the subsequent extinction [21–34]. In other words, the Allee effect is regarded as the reason for the increase in extinction risk at low densities [35].

Arsie et al. [21] studied a predator–prey model with Holling IV functional response and Allee effect in prey as follows:

$$\begin{aligned} \frac{dx}{dt} &= rx(\mathcal{K} - x)(x - A) - p(x)y, \\ \frac{dy}{dt} &= y(-d + cp(x)), \end{aligned} \tag{2}$$

where A represents the weak Allee effect or strong Allee effect in prey. The meaning of the other parameters is the same as those in model (1). Strong Allee effect takes place for $0 < A < \mathcal{K}$. On the other hand, the weak Allee effect never leads to negative growth when the weak Alee effect acts on predators or prey. The equilibrium of the system will change from asymptotically stable or central stable to unstable or central stable, or the system will take a longer time to reach the stable state, and this will take place for $-\mathcal{K} < A < 0$. $A = 0$ represents a threshold value between the strong and weak effects. Three limit cycles were found in predator–prey with the multiplicative Allee effect. Nilpotent cusp singularity of order 3 and degenerate Hopf bifurcation of codimension 3 are analyzed. An unfolding of the nilpotent saddle of codimension 3 was fully developed, indicating the existence of a heteroclinic cycle. However, the coexistence region of three limit cycles is still open.

Recently, the existence and generating mechanism of multiple limit cycles has attracted a lot of attention [21, 25, 36, 37]. Three limit cycles are found in Aguirre et al. [36], the first two are generated by Hopf bifurcation and the third one arises from a homoclinic bifurcation. The limit cycles are generated from different equilibria. Arsie et al. [21] also obtained three limit cycles which are originating from one Hopf bifurcation point. However, the true mechanism of the three limit cycles is not fully revealed, including the coexistence parameter region for the three limit cycles and the bifurcation characteristic of the limit cycle.

Group defense is also a type of anti-predator behavior. It represents the phenomenon that predators decrease because the prey has an increased ability to defend when their number is large enough [10]. Holling type IV has been used to study the phenomenon of prey aggregation, which can increase caution and decrease the chance of being attacked by the predator. Different species use their own defense mechanisms to fight, kill or escape from predators, and each of them shows its unique defense mechanism to avoid predation. It seems that the predator–prey relationship between organisms was established long ago. However, there are also some special predation phenomena in nature. Rodents can be eaten by snakes as prey and sometimes attack and eat snakes as predators. Moreover, some large groups of beasts hunt each other and some juvenile prey can escape from predation, when they become adults can counterattack juvenile predators such as alligators used to hunt catfish but adult catfish can eat alligator seedlings. Recognizing the effects of the anti-predator on reproduction, conservation, and behavior of the species has attracted a lot of attention in recent years. The detailed analysis and deep understanding of this phenomenon can bring important benefits not only for ecology but also for various applied disciplines including fishing and forestal industries. There are many examples of role reversals in predators and prey (anti-predator behaviors) [38–41].

Here we study a predator–prey model including the Holling IV response, strong and weak Allee effects in prey, and anti-predator behavior.

$$\begin{aligned} \frac{dx}{dt} &= rx(\mathcal{K}-x)(x-A) - p(x)y, \\ \frac{dy}{dt} &= y(-d+cp(x)) - \eta xy, \end{aligned} \tag{3}$$

where ηxy represents the interaction of the anti-predator behavior. The meaning of the rest of the parameters is the same as those in model (2).

Using

$$(t, x, y) \to \left(\frac{m^2c^2}{r}t, \frac{r}{mc}x, \frac{r}{mc^2}y\right),$$

system (3) becomes

$$\begin{aligned} \frac{dx}{dt} &= x(\mathcal{K}-x)(x-A) - p(x)y \triangleq p(x)(G(x)-y), \\ \frac{dy}{dt} &= y(-d+p(x)-\eta x), \end{aligned} \tag{4}$$

in which $p(x)$ is $\frac{x}{ax^2+bx+1}$ and $G(x)$ is $(x-A)(\mathcal{K}-x)(ax^2+bx+1)$ with

$$(\mathcal{K}, A, a, b, d, \eta) \to \left(\frac{mc}{r}\mathcal{K}, \frac{mc}{r}A, \frac{m^2c^2}{r^2}a, \frac{mc}{r}b, \frac{r}{m^2c^2}d, \frac{1}{mc}\eta\right).$$

In view of weak and strong Allee effects, here we set $-\mathcal{K} < A < \mathcal{K}$. In addition, since $ax^2+bx+1 > 0$ and $p(x) > 0$ for all $x > 0$, then we have $b > -2\sqrt{a}$. Denote

$$\Gamma = \{(\mathcal{K}, a, d, \eta, A, b) : -\mathcal{K} < A < \mathcal{K}, b > -2\sqrt{a}, a > 0, d > 0, \eta > 0\}.$$

We can find a constant $M > 0$ such that for every (x, y) in the set

$$\{(x, y) | x \geq 0, y \geq 0, p(x) < dy, x + y = N, N \geq M\},$$

one yields

$$\frac{dx}{dt} + \frac{dy}{dt} = p(x)G(x) - dy - \eta xy < p(x)G(x) - dy < 0.$$

All the orbits in the phase plane of model (4) will remain in a compact set enclosed by the x-axis, y-axis, and $x + y = M$.

In this paper, we study the complex dynamics of model (4) with the Holling IV response, strong and weak Allee effects, and anti-predator behavior. Detailed bifurcation analysis including saddle-node bifurcation, Bogdanov–Taken bifurcation of codimensions 2 and 3, Hopf bifurcation of codimension 3, saddle-node bifurcation of limit cycle, and codimension-2 cusp of limit cycle is derived.

The rest of the paper is structured as follows. In Sect. 2, the existence and stability of the equilibrium of model (4) are presented. In Sect. 3, we discuss saddle-node bifurcation and the cusp type of Bogdanov–Taken bifurcation of codimension 3. We prove the degenerate Hopf bifurcation of codimension 3 and show the coexistence of three limit cycles originating from a Hopf bifurcation point. Further, the normal form of codimension-2 cusp of limit cycle is revisited in Sect. 4. Numerical simulations are performed to illustrate the theoretical results in Sect. 5. Some biological interpretations of the bifurcation diagram and phase portrait exhibiting the significance of the Allee effect and anti-predate behavior are given in Sect. 6. Some conclusions and discussions are given at the end.

2 Local Stability Analysis

2.1 Number of Equilibria

System (4) always has one trivial equilibrium $E_0(0, 0)$ on the nonnegative x-axis and two boundary equilibria $E_K(K, 0)$ and $E_A(A, 0)$ representing, respectively, the extinction of predator and the threshold of Allee effect.

It s easy to see that $p(x) = d + \eta x$ if and only if $h(x)$ is zero, where

$$h(x) \triangleq a\eta x^3 + x^2(ad + b\eta) + x(bd + \eta - 1) + d. \tag{5}$$

We get the derivative function of $h(x)$ as follows

$$h'(x) = 2x(ad + b\eta) + 3a\eta x^2 + bd + \eta - 1. \tag{6}$$

The corresponding roots of equation (6) are

$$\begin{aligned} x_1 &= \frac{-\sqrt{\Delta} - 2(ad + b\eta)}{6a\eta}, \\ x_2 &= \frac{\sqrt{\Delta} - 2(ad + b\eta)}{6a\eta}, \\ \Delta &= 4(ad + b\eta)^2 - 12a\eta(bd + \eta - 1). \end{aligned}$$

From (5) and (6), we know that $h(0) = d > 0$.

Proposition 2.1 *By analyzing the derivative function of the $h(x)$, we obtain the existence of the root of $h(x)$.*

(I) *If* $\Delta \le 0$ *or* $\Delta > 0$ *and* $x_2 \le 0$, *then* $h(x)$ *has no real roots, i.e., system* (4) *has no equilibria;*

(II) *If* $\Delta > 0$ *and* $x_2 > 0$, *we have the following cases.*

(i) *if* $h(x_2) < 0$, *then* $h(x)$ *has two real roots, i.e., system* (4) *has two equilibrium points* $E_\alpha(x_\alpha, G(x_\alpha))$ *and* $E_\beta(x_\beta, G(x_\beta))$, *where* E_α *is a node or focus and* E_β *is a hyperbolic saddle;*

(ii) *if* $h(x_2) = 0$, *then* $h(x)$ *has one real root, i.e., system* (4) *has a unique positive equilibrium* $E_*(x_*, y_*)$, *which is a degenerate equilibrium;*

(iii) *if* $h(x_2) > 0$, *then* $h(x)$ *has no real root, i.e., system* (4) *has no positive equilibrium.*

Proof Since the function $h'(x)$ is a continuous function, $h'(x) > 0$ is forever admitted as $\Delta \le 0$ or $\Delta > 0$ and $x_2 \le 0$. Thus, $h(x)$ is monotonically increasing. In view of $h(0) = d > 0$, $h(x)$ has no real roots.

When $\Delta > 0$ and $x_1 < 0 < x_2$, $h'(x) < 0$ as $x \in (0, x_2)$, $h'(x) > 0$ as $x \in (x_2, +\infty)$. Moreover, when $\Delta > 0$ and $0 < x_1 < x_2$, $h'(x) < 0$ as $x \in (x_1, x_2)$, $h'(x) > 0$ as $x \in (0, x_1) \cup (x_2, +\infty)$. In these two situations, we will have two real roots of $h(x)$ if $h(x_2) < 0$ which are denoted by α and β. Thus, system (4) has two positive equilibria $E_\alpha(x_\alpha, G(x_\alpha))$ and $E_\beta(x_\beta, G(x_\beta))$. It has one unique root if $h(x_2) = 0$ which is denoted by x_*. In this case, system (4) has a unique positive equilibrium $E_*(x_*, y_*)$. We also notice that $x_* = x_2$ in this situation. There is no real root if $h(x_2) > 0$. See Fig. 1.

$$h(x_2) = \frac{1}{27a^2\eta^2}(27a^2d\eta^2 + 3M^2(ad + b\eta) + 9a\eta M(bd + \eta - 1) + M^3),$$
$$M = \sqrt{(ad + b\eta)^2 - 3a\eta(bd + \eta - 1)} - ad - b\eta.$$

Moreover, the Jacobian matrix of system (4) at any equilibrium $E(x, y)$ takes the form

$$J(E) = \begin{pmatrix} \frac{x\left(\mathcal{K}+A\left(3ax^2+2bx-(b+2ax)\mathcal{K}+1\right)+x(b(2\mathcal{K}-3x)+ax(3\mathcal{K}-4x)-2)\right)}{x(b+ax)+1} & -\frac{x}{x(b+ax)+1} \\ \frac{(A-x)(x-\mathcal{K})\left(-ax^2-(x(b+ax)+1)^2\eta+1\right)}{x(b+ax)+1} & 0 \end{pmatrix}, \tag{7}$$

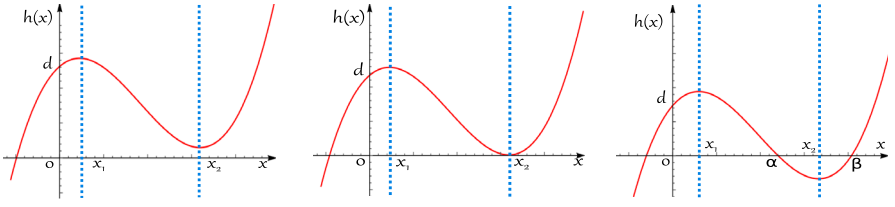

Fig. 1 The distribution of roots of $h(x)$ as $\Delta > 0$, $x_1 > 0$ and $x_2 > 0$.

and

$$\det(J(E)) = \frac{x(x-A)(x-\mathcal{K})\left(\eta(x(ax+b)+1)^2+ax^2-1\right)}{(x(ax+b)+1)^2},$$
$$\mathrm{tr}(J(E)) = \frac{x\left(A\left(-\mathcal{K}(2ax+b)+3ax^2+2bx+1\right)+x(ax(3\mathcal{K}-4x)+b(2\mathcal{K}-3x)-2)+\mathcal{K}\right)}{x(ax+b)+1}.$$

We can rewrite $\det(J(E))$ as

$$\det(J(E)) = \frac{x(x-A)(x-\mathcal{K})\left(h'(x)\left(ax^2+bx+1\right)+h(x)(-2ax-b)\right)}{(ax^2+bx+1)^2}. \tag{8}$$

Since $x(x-A)(\mathcal{K}-x) > 0$, the positive equilibrium $E_\alpha(x_\alpha, G(x_\alpha))$ is a node or focus and the positive equilibrium $E_\beta(x_\beta, G(x_\beta))$ is a hyperbolic saddle. □

2.2 Linear Analysis

Define

$$\begin{aligned} d_* &= \frac{x_*^2(2ax_*+b)}{(x_*(ax_*+b)+1)^2},\\ \eta_* &= \frac{1-ax_*^2}{(x_*(ax_*+b)+1)^2},\\ \mathcal{K}_* &= \frac{A^2(-(x_*(ax_*+b)+1))+Ax_*\left(ax_*^2+2bx_*+3\right)+x_*^2\left(ax_*^2-1\right)}{x_*\left(-A(2ax_*+b)+3ax_*^2+2bx_*+1\right)}, \end{aligned} \tag{9}$$

which come from $h(x_*) = 0$, $h'(x_*) = 0$ and $\mathrm{tr}(J(E_*)) = 0$, respectively.

Using (9), we obtain that the possible equilibrium of system (4) is

$$E(x_*, G(x_*)) = (x_*, \frac{(A-2x_*)(A-x_*)^2(x_*(ax_*+b)+1)^2}{x_*(x_*(-2aA+3ax_*+2b)-Ab+1)}).$$

Proposition 2.2 *When $(a, A, b, d, \eta, \mathcal{K}) \in \Gamma$, and $h(x) = 0$, there exists a unique positive equilibrium $E_*(x_*, y_*)$ for system (4). Furthermore,*

(I) *if $\mathcal{K} \neq \mathcal{K}_*$, then $E_*(x_*, y_*)$ is a saddle-node. It has a stable parabolic sector (or an unstable parabolic sector) if $\mathcal{K} > \mathcal{K}_*$ (or $\mathcal{K} < \mathcal{K}_*$);*
(II) *if $\mathcal{K} = \mathcal{K}_*$, d_*, η_*, $\mathcal{K}_*$ are defined by (9), then $E_*(x_*, y_*)$ is a cusp. Moreover,*
(i) *if $A \neq A_*$, then $E_*(x_*, y_*)$ is a cusp of codimension 2;*
(ii) *if $A = A_*$, then $E_*(x_*, y_*)$ is a cusp of codimension 3.*

Proof The assertion (I) is proved in Xiao and Zhou [42] (see Lemma 2.7).

In the following, we prove that the degenerate equilibrium $E_*(x_*, y_*)$ is a codimension-2 cusp.

Let X be $x - x_*$, Y be $y - y_*$, and $dt = -\frac{ax_*^2+bx_*+1}{x_*}d\tau$, $d = d_*$, $\mathcal{K} = \mathcal{K}_*$ and $\eta = \eta_*$. By Taylor expansion, model (4) becomes

$$\begin{aligned}\frac{dx}{dt} &= y + \alpha_1 x^2 + \alpha_2 xy + o(|x, y)|^2),\\ \frac{dy}{dt} &= \alpha_3 x^2 + o(|x, y|^2),\end{aligned} \tag{10}$$

where

$$\begin{aligned}\alpha_1 &= \frac{3bx_*\left(aA^2 - Ab + 1\right)}{-A\left(2ax_* + b\right) + 3ax_*^2 + 2bx_* + 1} + \frac{1 - A\left(aA - Ab^2 + b\right)}{-A\left(2ax_* + b\right) + 3ax_*^2 + 2bx_* + 1}\\ &\quad + \frac{3x_*^2\left(a^2A^2 - 3aAb + a + b^2\right)}{-A\left(2ax_* + b\right) + 3ax_*^2 + 2bx_* + 1} + \frac{6a^2x_*^4 + 8ax_*^3(b - aA)}{-A\left(2ax_* + b\right) + 3ax_*^2 + 2bx_* + 1},\\ \alpha_2 &= \frac{1}{x_*\left(ax_*^2 + bx_* + 1\right)} - \frac{ax_*}{ax_*^2 + bx_* + 1},\\ \alpha_3 &= \frac{(A - x_*)^2\left(a^2x_*^3 - 3ax_* - b\right)}{x_*\left(2aAx_* - 3ax_*^2 + Ab - 2bx_* - 1\right)}.\end{aligned}$$

By using Remark 1 of section 2.13 in Perko [43] (also in Huang et al. [39]), near (0, 0) model (10) is equivalent to

$$\begin{aligned}\frac{dx}{dt} &= y + o(|x, y)|^2),\\ \frac{dy}{dt} &= \alpha_3 x^2 + 2\alpha_1 xy + o(|x, y|^2).\end{aligned} \tag{11}$$

Then $E_*(x_*, y_*)$ is a cusp of codimension 2.

Next, we prove the assertion (ii) of (II). Define

$$A_* = \frac{8a^2x_*^3 + \sqrt{-(x_*(ax_* + b) + 1)^2\left(4a\left(2x_*(ax_* + b) - 1\right) + 3b^2\right)} + 9abx_*^2 + 3b^2x_* + b}{2\left(a\left(3x_*(ax_* + b) - 1\right) + b^2\right)}, \tag{12}$$

which leads to $\alpha_1 = 0$. Using Taylor expansion, system (4) can be written as (for simplicity, we still denote X, Y, τ by x, y, t, respectively)

$$\begin{aligned}\frac{dx}{dt} &= y + \beta_1 x^2 + \beta_2 xy + \beta_3 x^3 + \beta_4 x^2 y + \beta_5 x^4 + \beta_6 x^3 y + o(|x, y)|^4),\\ \frac{dy}{dt} &= \beta_7 x^2 + \beta_8 x^3 + \beta_9 x^2 y + \beta_{10} x^4 + \beta_{11} x^3 y + o(|x, y|^4),\end{aligned} \tag{13}$$

where

$$\beta_1 = 0, \beta_2 = \frac{1}{x_*\left(ax_*^2 + bx_* + 1\right)} - \frac{ax_*}{ax_*^2 + bx_* + 1},$$
$$\beta_3 = \frac{4a^3x_*^3 + 6a^2bx_*^2 - 4a^2x_* + 4ab^2x_* - 2ab + b^3}{3a^2x_*^2 + 3abx_* - a + b^2}, \beta_4 = \frac{a^2x_*^3 - 3ax_* - b}{x_*\left(ax_*^2 + bx_* + 1\right)^2},$$
$$\beta_5 = \frac{-a^4x_*^5 + 10a^3x_*^3 + 10a^2bx_*^2 - 5a^2x_* + 5ab^2x_* - 2ab + b^3}{x_*\left(ax_*^2 + bx_* + 1\right)\left(3a^2x_*^2 + 3abx_* - a + b^2\right)},$$

$$\beta_6 = \frac{-a^3x_*^4 + 6a^2x_*^2 + 4abx_* - a + b^2}{x_*\left(ax_*^2 + bx_* + 1\right)^3}, \beta_7 = \frac{\left(ax_*^2 + bx_* + 1\right)\left(a^2x_*^3 - 3ax_* - b\right)}{x_*\left(3a^2x_*^2 + 3abx_* - a + b^2\right)},$$
$$\beta_8 = \frac{-a^3x_*^4 + 6a^2x_*^2 + 4abx_* - a + b^2}{x_*\left(3a^2x_*^2 + 3abx_* - a + b^2\right)}, \beta_9 = \frac{-a^2x_*^3 + 3ax_* + b}{x_*\left(ax_*^2 + bx_* + 1\right)^2},$$
$$\beta_{10} = \frac{a^4x_*^5 - 10a^3x_*^3 - 10a^2bx_*^2 + 5a^2x_* - 5ab^2x_* + 2ab - b^3}{x_*\left(ax_*^2 + bx_* + 1\right)\left(3a^2x_*^2 + 3abx_* - a + b^2\right)},$$
$$\beta_{11} = \frac{a^3x_*^4 - 6a^2x_*^2 - 4abx_* + a - b^2}{x_*\left(ax_*^2 + bx_* + 1\right)^3},$$

where d, $\mathcal{K}$ and η have been eliminated by (9).
We use the transformation

$$X = x,$$
$$Y = y + \beta_1x^2 + \beta_2xy + \beta_3x^3 + \beta_4x^2y + \beta_5x^4 + \beta_6x^3y + o(|x, y|^4),$$

that changes (13) to (still use x, y for X, Y; for simplicity we always did this after the transformation)

$$\begin{aligned}\frac{dx}{dt} &= y,\\ \frac{dy}{dt} &= \gamma_1x^2 + \gamma_2y^2 + \gamma_3x^3 + \gamma_4x^2y + \gamma_5xy^2 + \gamma_6x^4 + \gamma_7x^3y + \gamma_8x^2y^2 + o(|x, y)|^4),\end{aligned} \tag{14}$$

where γ_i, $(i = 1, \ldots, 8)$ are given in "Appendix A".

In addition, letting $dt = (1 - \gamma_2x)d\tau$, system (14) becomes (we still denote τ by t, respectively)

$$\begin{aligned}\frac{dx}{dt} &= y(1 - \gamma_2x),\\ \frac{dy}{dt} &= (1 - \gamma_2x)(\gamma_1x^2 + \gamma_2y^2 + \gamma_3x^3 + \gamma_4x^2y + \gamma_5xy^2\\ &\quad + \gamma_6x^4 + \gamma_7x^3y + \gamma_8x^2y^2 + o(|x, y|^4)).\end{aligned} \tag{15}$$

Letting $X = x$, $Y = y(1 - \gamma_2 x)$, system (15) becomes

$$\begin{aligned}\frac{dx}{dt} &= y,\\ \frac{dy}{dt} &= \gamma_1 x^2 + (-2\gamma_1\gamma_2)x^3 + \gamma_4 x^2 y + (-\gamma_2^2 + \gamma_5)xy^2\\ &\quad + (\gamma_2\gamma_2^2 - 2\gamma_2\gamma_3 + \gamma_6)x^4 + (-\gamma_2\gamma_4 + \gamma_7)x^3 y + (-\gamma_2^3 + \gamma_8)x^2 y^2 + o(|x, y|^4).\end{aligned} \tag{16}$$

Using the transformation

$$X = -x, \quad Y = -\frac{y}{\sqrt{-\gamma_1}} \quad \tau = \sqrt{-\gamma_1}t,$$

we obtain

$$\begin{aligned}\frac{dx}{dt} &= y,\\ \frac{dy}{dt} &= x^2 + 2\gamma_2 x^3 + \left(-\frac{\sqrt{-\gamma_1}\gamma_4}{\gamma_1}\right)x^2 y + (-\gamma_2^2 + \gamma_5)xy^2\\ &\quad + \left(\frac{\gamma_1\gamma_2^2 - 2\gamma_3\gamma_2 + \gamma_6}{\gamma_1}\right)x^4 + \left(\frac{\sqrt{-\gamma_1}\gamma_7}{\gamma_1} - \frac{\sqrt{-\gamma_1}\gamma_2\gamma_4}{\gamma_1}\right)x^3 y\\ &\quad + (\gamma_2^3 - \gamma_8)x^2 y^2 + o(|x, y|^4).\end{aligned} \tag{17}$$

By Proposition 5.3 in Lamontagne et al. [44], we obtain the equivalent system of (17) as follows:

$$\begin{aligned}\frac{dx}{dt} &= y,\\ \frac{dy}{dt} &= x^2 + Gx^3 y + o(|x, y|^4),\end{aligned} \tag{18}$$

where

$$\begin{aligned}G &= -\frac{\sqrt{\frac{(x_*(ax_*+b)+1)(ax_*(3-ax_*^2)+b)}{x_*(a(3x_*(ax_*+b)-1)+b^2)}}}{x_*\left(x_*\left(ax_*+b\right)+1\right)^4\left(ax_*\left(ax_*^2-3\right)-b\right)}T \neq 0,\\ T &= 12a^6x_*^{10} + 36a^5bx_*^9 + x_*^2\left(-20a^2b + 28a^2 + 8ab^3 - 4ab^2 - 12b^4\right)\\ &\quad + x_*^8\left(44a^4b^2 - 32a^5\right)\\ &\quad + x_*\left(4a^2 - 8ab^2 + 12ab + b^4 - 6b^3\right)\\ &\quad + x_*^3\left(-22a^3 + 28a^2b^2 + 24a^2b - 54ab^3 - 6b^5\right)\\ &\quad + x_*^4\left(45a^3b - 108a^2b^2 - 36ab^4\right)\end{aligned}$$

$$+x_*^6\left(-6a^4b-72a^4-156a^3b^2+12a^2b^4\right)+ab-b^3$$
$$+x_*^7\left(-6a^5-120a^4b+30a^3b^3\right)$$
$$+x_*^5\left(32a^4-2a^3b^2-144a^3b-98a^2b^3+2ab^5\right)$$

and A has been eliminated by (12).
Thus, system (4) undergoes a cusp bifurcation of codimension 3. □

Proposition 2.3 *When $\Delta > 0$, $x_2 > 0$ and $h(x_2) < 0$ are satisfied, there are two positive equilibria $E_\alpha(x_\alpha, y_\alpha)$ and $E_\beta(x_\beta, y_\beta)$ for system (4). Further, E_β is a hyperbolic saddle and E_α is*

(i) *a stable hyperbolic focus or node when $S_T(\alpha) < 0$;*
(ii) *a weak focus or a center when $S_T(\alpha) = 0$;*
(iii) *an unstable hyperbolic focus or node when $S_T(\alpha) > 0$.*

Proof Denote the sign of the determinant and trace of (7) by

$$S_D(x) = x(x-A)(x-\mathcal{K})\left(ax^2+\eta(x(ax+b)+1)^2-1\right),$$
$$S_T(x) = A\left(-\mathcal{K}(2ax+b)+3ax^2+2bx+1\right)$$
$$+x(ax(3\mathcal{K}-4x)+b(2\mathcal{K}-3x)-2)+\mathcal{K}.$$

Substituting α and β into $S_D(x)$, we have

$$S_D(\alpha) = \alpha(\alpha-A)(\alpha-\mathcal{K})\left(a\alpha^2+\eta(\alpha(a\alpha+b)+1)^2-1\right),$$
$$S_D(\beta) = \beta(\beta-A)(\beta-\mathcal{K})\left(a\beta^2+\eta(\beta(a\beta+b)+1)^2-1\right).$$

Note that, we find that α and β are two different positive roots of (5), then

$$h'(\alpha) = -a\alpha^2-\eta(\alpha(a\alpha+b)+1)^2+1<0. \tag{19}$$
$$h'(\beta) = -a\beta^2-\eta(\beta(a\beta+b)+1)^2+1>0. \tag{20}$$

From model (4), we have

$$x(\mathcal{K}-x)(x-A)>0.$$

It follows that $S_D(\alpha) > 0$ and $S_D(\beta) < 0$ by (19) and (20). Hence we obtain the types of E_α and E_β. □

3 Bifurcation Analysis

In this section, we discuss the existence of saddle-node bifurcation, Hopf bifurcation of codimensions 3, Bogdanov–Takens bifurcation of codimensions 2 and 3 by the method of normal form theory.

3.1 Saddle-Node Bifurcation

From the last section, we obtain that two positive equilibria of system (4) will coincide at $E(\tilde{x})$ which leads to $h(\tilde{x}) = h'(\tilde{x}) = 0$. Moreover, from (8), there may exist saddle-node bifurcation of system (4).

Theorem 3.1 *Suppose $h(\tilde{x}) = h'(\tilde{x}) = 0$. If $r(\tilde{x}_*) \neq 0$, then system (4) goes through a saddle-node bifurcation.*

Proof Since $h(\tilde{x}) = h'(\tilde{x}) = 0$, the eigenvalues of $J(\tilde{E})$ are 0 and $-r(\tilde{x})$. From (8), we have $\det(\tilde{E}) = 0$. We use the following transformation to show that system (4) undergoes a saddle-node bifurcation.

From (9), we have $\tilde{d} = \frac{\tilde{x}^2(2a\tilde{x}+b)}{(\tilde{x}(a\tilde{x}+b)+1)^2}$, $\tilde{\eta} = \frac{1-a\tilde{x}^2}{(\tilde{x}(a\tilde{x}+b)+1)^2}$. Bringing $\tilde{E}$ to the origin by the transformation $\tilde{X} = x - \tilde{x}$, $\tilde{Y} = y - \tilde{y}$, system (4) becomes (we still denote $\tilde{X}$, $\tilde{Y}$ as $\tilde{x}$, $\tilde{y}$, respectively)

$$\begin{aligned} \frac{d\tilde{x}}{dt} &= \delta_1 x + \delta_2 y + \delta_3 xy + \delta_4 x^2 + \delta_5 x^3 + \delta_6 x^2 y + O(|\tilde{x}, \tilde{y}|^4), \\ \frac{d\tilde{y}}{dt} &= \delta_7 x^2 + \delta_8 x^3 + \delta_9 x^2 y + O(|\tilde{x}, \tilde{y}|^4), \end{aligned} \tag{21}$$

where δ_i, $(i = 1, \ldots, 9)$ are given in "Appendix B".

Next, using the transformation

$$\begin{aligned} X &= \tilde{y}, \\ Y &= (x_* \left(-3x_*(a(A+\mathcal{K}) - b) + 2aA\mathcal{K} + 4ax_*^2 - 2Ab - 2b\mathcal{K} + 2\right) \\ &\quad + A(b\mathcal{K} - 1) - \mathcal{K})\tilde{x} + \tilde{y}, \end{aligned}$$

system (21) becomes

$$\begin{aligned} \frac{dX}{dt} &= \epsilon_1 X^2 + \epsilon_2 X^3 + \epsilon_3 X^2 Y + O(|X, Y|^4), \\ \frac{dY}{dt} &= -r(x_*)Y + \epsilon_4 X^2 + \epsilon_5 XY + \epsilon_6 X^3 + \epsilon_7 X^2 Y + O(|X, Y|^4), \end{aligned} \tag{22}$$

where ϵ_i, $(i = 1, \ldots, 7)$ and $r(x_*)$ are, respectively, defined in "Appendix C".

There exists the following center manifold in a sufficiently small neighborhood of the origin $(0, 0)$

$$Y = \frac{\epsilon_4}{r(x_*)} X^2 + O(X^3).$$

System (22) can be reduced on this center manifold as follows:

$$\frac{dX}{dt} = \epsilon_2 X^2 + O(X^3). \tag{23}$$

Due to $\epsilon_2 \neq 0$, system (23) is topologically equivalent to

$$\frac{dX}{dt} = \pm X^2 + O(X^3).$$

Then system (4) goes through a saddle-node bifurcation based on Shan and Zhu [45]. □

3.2 Bogdanov–Takens Bifurcation of Codimensions Two and Three

In this subsection, we consider the codimension-2 and codimension-3 Bogdanov–Takens bifurcation of system (4) using the method of finding the parametric normal form of Bogdanov–Takens bifurcation, which was developed by Dumortier et al. [46]. Here we use the natural mortality rate (d) of the predator, the prey's carrying capacity ($\mathcal{K}$), and the intensity of anti-predator behavior (η) as the primary bifurcation parameters.

Firstly, we recall the following definition in Perko [43] and proposition in Li et al. [37] which will be used in our proof.

Definition 3.1 The bifurcation that results from unfolding the following normal form of a cusp of codimension 3,

$$\begin{aligned} \frac{dx}{dt} &= y, \\ \frac{dy}{dt} &= x^2 \pm x^3 y, \end{aligned} \tag{24}$$

is called a cusp type degenerate Bogdanov–Takens bifurcation of codimension 3.

Proposition 3.1 *A universal unfolding of the normal form* (24) *is expressed by*

$$\begin{cases} \frac{dx}{dt} = y, \\ \frac{dy}{dt} = \nu_1 + \nu_2 y + \nu_3 xy + x^2 \pm x^3 y + R(x, y, \varepsilon), \end{cases} \tag{25}$$

where $\varepsilon = (\varepsilon_1, \varepsilon_2, \varepsilon_3) \sim (0, 0, 0)$, $\frac{D(\nu_1, \nu_2, \nu_3)}{D(\varepsilon_1, \varepsilon_2, \varepsilon_3)} \neq 0$ *for small* ε *and*

$$\begin{aligned} R(x, y, \varepsilon) = {} & y^2 O(|x, y|^2) + O(|x, y|^5) + O(\varepsilon)(O(y^2) + O(|x, y|^3)) \\ & + O(\varepsilon^2) O(|x, y|). \end{aligned} \tag{26}$$

Theorem 3.2 *When* $d = d_* = fracx_*^2 (2ax_* + b)(x_* (ax_* + b) + 1)^2$, $\eta = \eta_* = \frac{1 - ax_*^2}{(x_*(ax_* + b) + 1)^2}$, $\mathcal{K} = \mathcal{K}_*$ *which are mentioned in* (9), *system* (4) *has an interior equilibrium* $E(x_*, G(x_*))$ *which is a cusp of codimension-2 (i.e., B-T singularity). If we take* d *and* η *as bifurcation parameters and* $|\frac{\partial(\mu_1, \mu_2)}{\partial(\lambda_1, \lambda_2)}|_{\lambda=0} \neq 0$, *then system* (4) *goes through codimension-2 Bogdanov–Takens bifurcation in a small neighborhood of the*

unique positive equilibrium $E(x_*, G(x_*))$. Further, if we take d, η, $\mathcal{K}$ as the primary bifurcation parameters and $|\frac{\partial(\nu_1,\nu_2,\nu_3)}{\partial(\lambda_1,\lambda_2,\lambda_3)}|_{\lambda=0} \neq 0$, then system (4) undergoes codimension-3 Bogdanov–Taken bifurcation in a small neighborhood of the positive equilibrium $E(x_*, G(x_*))$. Then we find an unstable homoclinic cycle, a stable limit cycle, coexistence of two limit cycles, and a semi-stable limit cycle for different intervals of parameter values for system (4).

Proof We prove codimension-2 Bogdanov–Takens bifurcation by using d and η as primary bifurcation parameters.
Set

$$\begin{aligned}\frac{dx}{dt} &= x(x-A)(\mathcal{K}-x) - \frac{xy}{ax^2+bx+1},\\ \frac{dy}{dt} &= y\left(\frac{x}{ax^2+bx+1} - (d+\lambda_1) + x\left(-(\eta+\lambda_2)\right)\right),\end{aligned} \tag{27}$$

where λ_1 and λ_2 are small parameters near $(0, 0)$. We are only interested in the phase portrait of model (27) in a small neighborhood of $E_*(x_*, y_*)$.

Let $X = x - x_*$, $Y = y - y_*$. Model (27) can be written as

$$\begin{aligned}\frac{dx}{dt} &= \varepsilon_1 + \varepsilon_2 x + \varepsilon_3 y + \varepsilon_4 x^2 + \varepsilon_5 xy + P_1(x, y, \lambda_1, \lambda_2),\\ \frac{dy}{dt} &= \varepsilon_6 + \varepsilon_7 x + \varepsilon_8 y + \varepsilon_9 x^2 + \varepsilon_{10} xy + P_2(x, y, \lambda_1, \lambda_2),\end{aligned} \tag{28}$$

where $P_1(x, y, \lambda_1, \lambda_2)$ and $P_2(x, y, \lambda_1, \lambda_2)$ are functions which has at least third derivative about (x, y). The coefficients depend smoothly on λ_1 and λ_2, and

$$\begin{aligned}
&\varepsilon_1 = \varepsilon_2 = 0, \qquad \varepsilon_3 = -\frac{x_*}{ax_*^2+bx_*+1},\\
&\varepsilon_4 = \frac{(A-x_*)^2\left(a^2x_*^3 - 3ax_* - b\right)}{\left(ax_*^2+bx_*+1\right)\left(2aAx_* - 3ax_*^2 + Ab - 2bx_* - 1\right)}\\
&\qquad + \frac{(A-x_*)\left(x_*(ax_*+b)+1\right)}{x_*(2aA - 3ax_* - 2b) + Ab - 1} + A - 2x_*,\\
&\varepsilon_5 = \frac{ax_*^2 - 1}{\left(ax_*^2+bx_*+1\right)^2}, \qquad \varepsilon_6 = \frac{(A-x_*)^2(\lambda_1+\lambda_2 x_*)\left(ax_*^2+bx_*+1\right)^2}{2aAx_* - 3ax_*^2 + Ab - 2bx_* - 1},\\
&\varepsilon_7 = \frac{\lambda_2(A-x_*)^2\left(ax_*^2+bx_*+1\right)^2}{2aAx_* - 3ax_*^2 + Ab - 2bx_* - 1}, \qquad \varepsilon_8 = -\lambda_1 - \lambda_2 x_*,\\
&\varepsilon_9 = -\frac{(A-x_*)^2\left(a^2x_*^3 - 3ax_* - b\right)}{\left(ax_*^2+bx_*+1\right)\left(2aAx_* - 3ax_*^2 + Ab - 2bx_* - 1\right)}, \qquad \varepsilon_{10} = -\lambda_2.
\end{aligned}$$

Let $X = x, Y = \varepsilon_1 + \varepsilon_2 x + \varepsilon_3 y + \varepsilon_4 x^2 + \varepsilon_5 xy + P_1(x, y, \lambda_1, \lambda_2)$. Model (28) reduces to

$$\begin{aligned}\frac{dx}{dt} &= y,\\ \frac{dy}{dt} &= \zeta_1 + \zeta_2 x + \zeta_3 y + \zeta_4 x^2 + \zeta_5 xy + \zeta_6 y^2 + P_3(x, y, \lambda_1, \lambda_2),\end{aligned} \tag{29}$$

where $P_3(x, y, \lambda_1, \lambda_2)$ is a function which has at least third derivative about (x, y). The corresponding coefficients depend smoothly on λ_1 and λ_2, and

$$\zeta_1 = \varepsilon_3\varepsilon_6 - \varepsilon_1\varepsilon_8, \zeta_2 = \varepsilon_5\varepsilon_6 + \varepsilon_3\varepsilon_7 - \varepsilon_2\varepsilon_8 - \varepsilon_1\varepsilon_{10}, \zeta_3 = \varepsilon_2 + \varepsilon_8 - \frac{\varepsilon_1\varepsilon_5}{\varepsilon_3},$$

$$\zeta_4 = \varepsilon_5\varepsilon_7 - \varepsilon_4\varepsilon_8 + \varepsilon_3\varepsilon_9 - \varepsilon_2\varepsilon_{10}, \zeta_5 = \frac{\varepsilon_1\varepsilon_5^2}{\varepsilon_3^2} - \frac{\varepsilon_2\varepsilon_5}{\varepsilon_3} + 2\varepsilon_4 + \varepsilon_{10}, \zeta_6 = \frac{\varepsilon_5}{\varepsilon_3}.$$

Next, let $dt = (1 - \zeta_6 x)d\tau$. System (29) becomes (still denote τ by t, respectively)

$$\begin{aligned}\frac{dx}{dt} &= y(1 - \zeta_6 x),\\ \frac{dy}{dt} &= (1 - \zeta_6 x)(\zeta_1 + \zeta_2 x + \zeta_3 y + \zeta_4 x^2 + \zeta_5 xy + \zeta_6 y^2 + P_3(x, y, \lambda_1, \lambda_2)).\end{aligned} \tag{30}$$

Let $X = x$, $Y = y(1 - \zeta_6 x)$, and rewrite X, Y as x, y, respectively, one yields

$$\begin{aligned}\frac{dx}{dt} &= y,\\ \frac{dy}{dt} &= \theta_1 + \theta_2 x + \theta_3 y + \theta_4 x^2 + \theta_5 xy + P_4(x, y, \lambda_1, \lambda_2)),\end{aligned} \tag{31}$$

where $P_4(x, y, \lambda_1, \lambda_2)$ is a function which has at least third derivative about (x, y). We have

$$\theta_1 = \zeta_1, \ \ \theta_2 = \zeta_2 - 2\zeta_1\zeta_6, \ \ \theta_3 = \zeta_3, \ \ \theta_4 = \zeta_1\zeta_6^2 - 2\zeta_2\zeta_6 + \zeta_4, \ \ \theta_5 = \zeta_5 - \zeta_3\zeta_6.$$

We find that when $\lambda_1 = \lambda_2 = 0$,

$$\theta_1 = \theta_2 = \theta_3 = 0,$$
$$\theta_4 = \frac{x_*\left(A - x_*\right)^2\left(ax_*\left(ax_*^2 - 3\right) - b\right)}{\left(x_*\left(ax_* + b\right) + 1\right)^2\left(A\left(2ax_* + b\right) - 3ax_*^2 - 2bx_* - 1\right)} \neq 0.$$

Moreover, let

$$X = \frac{\theta_2}{2\theta_4} + x, \quad Y = y.$$

Model (31) becomes

$$\begin{aligned} \frac{dx}{dt} &= y, \\ \frac{dy}{dt} &= \iota_1 + \iota_2 y + \iota_3 x^2 + \iota_4 xy + P_5(x, y, \lambda_1, \lambda_2)). \end{aligned} \tag{32}$$

Here $P_5(x, y, \lambda_1, \lambda_2)$ has at least third derivative about (x, y). We have

$$\iota_1 = \theta_1 - \frac{\theta_2^2}{4\theta_4}, \quad \iota_2 = \theta_3 - \frac{\theta_2\theta_5}{2\theta_4}, \quad \iota_3 = \theta_4, \quad \iota_4 = \theta_5.$$

Assuming

$$X = \frac{\iota_4^2}{\iota_3}x, \quad Y = \frac{\iota_4^3}{\iota_3^2}y, \quad \tau = \frac{\iota_3}{\iota_4}t,$$

we have (use x, y, t for X, Y, τ)

$$\begin{aligned} \frac{dx}{dt} &= y, \\ \frac{dy}{dt} &= \mu_1 + \mu_2 y + x^2 + xy + P_6(x, y, \lambda_1, \lambda_2)), \end{aligned} \tag{33}$$

where $P_6(x, y, \lambda_1, \lambda_2)$ has at least third derivative about (x, y). We have

$$\mu_1 = \frac{\iota_1\iota_4^4}{\iota_3^3}, \quad \mu_2 = \frac{\iota_2\iota_4}{\iota_3}.$$

We write μ_1 and μ_2 using λ_1 and λ_2

$$\begin{aligned} \mu_1 &= s_1\lambda_1 + s_2\lambda_2 + s_3\lambda_1^2 + s_4\lambda_1\lambda_2 + +s_5\lambda_2^2 + 0(|\lambda_1, \lambda_2|), \\ \mu_2 &= t_1\lambda_1 + t_2\lambda_2 + t_3\lambda_1^2 + t_4\lambda_1\lambda_2 + +t_5\lambda_2^2 + 0(|\lambda_1, \lambda_2|), \end{aligned} \tag{34}$$

Then it yields

$$\begin{aligned} \left|\frac{\partial(\mu_1, \mu_2)}{\partial(\lambda_1, \lambda_2)}\right| &= \frac{32R^6x_*^3\left(x_*\left(ax_*+b\right)+1\right)^6}{\left(A-x_*\right)^6\left(ax_*\left(ax_*^2-3\right)-b\right)^5\left(x_*\left(2aA-3ax_*-2b\right)+Ab-1\right)^3} \\ &\neq 0, \end{aligned}$$

where

$$\begin{aligned} R = {} & 3x_*^2\left(a^2A^2 - 3aAb + a + b^2\right) + x_*^3\left(8ab - 8a^2A\right) + 6a^2x_*^4 \\ & +3bx_*\left(aA^2 - Ab + 1\right) - aA^2 + Ab(Ab-1) + 1. \end{aligned}$$

Thus, system (4) undergoes a codimension-2 Bogdanov–Takens bifurcation.

Next, we take d, η, $\mathcal{K}$ as bifurcation parameters to prove that model (4) has a Bondanov-Takens bifurcation of codimension 3. Set

$$\begin{aligned}\frac{dx}{dt} &= x(x-A)\left((\lambda_3+\mathcal{K})-x\right)-\frac{xy}{ax^2+bx+1},\\ \frac{dy}{dt} &= y\left(\frac{x}{ax^2+bx+1}-(d+\lambda_1)+x\left(-(\eta+\lambda_2)\right)\right).\end{aligned} \tag{35}$$

Here λ_i $(i=1,2,3)$ is in a sufficiently small neighborhood of $(0,0)$. We are concerned about the dynamics of system (35) near the equilibrium $E_*(x_*, y_*)$.

Firstly, define $X = x - x_*$, $Y = y = y_*$. By using Taylor expansion, system (35) can be rewritten as (we still denote X, Y by x, y, respectively)

$$\begin{aligned}\frac{dx}{dt} &= a_{00}+a_{10}x+a_{01}y+a_{20}x^2+a_{11}xy+a_{30}x^3+a_{21}x^2y\\ &\quad +a_{40}x^4+a_{31}x^3y+O(|x,y|^4),\\ \frac{dy}{dt} &= r_{00}+r_{10}x+r_{01}y+r_{20}x^2+r_{11}xy+r_{30}x^3+r_{21}x^2y\\ &\quad +r_{40}x^4+r_{31}x^3y+O(|x,y|^4),\end{aligned} \tag{36}$$

where

$$a_{00}=\lambda_3x_*^2-A\lambda_3x_*,\ a_{10}=2\lambda_3x_*-A\lambda_3,\ a_{01}=-\frac{x_*}{ax_*^2+bx_*+1},\ a_{20}=\lambda_3,$$

$$a_{11}=\frac{ax_*^2-1}{\left(ax_*^2+bx_*+1\right)^2},\ a_{30}=-\frac{x_*\left(2ax_*+b\right)\left(2a\left(x_*\left(ax_*+b\right)-1\right)+b^2\right)}{\left(x_*\left(ax_*+b\right)+1\right)\left(a\left(3x_*\left(ax_*+b\right)-1\right)+b^2\right)},$$

$$a_{21}=\frac{-a^2x_*^3+3ax_*+b}{\left(ax_*^2+bx_*+1\right)^3},$$

$$a_{40}=\frac{x_*\left(b^2-4a\right)}{\left(x_*\left(ax_*+b\right)+1\right)^2}+\frac{a\left(ax_*+b\right)}{a\left(3x_*\left(ax_*+b\right)-1\right)+b^2}-\frac{b}{x_*\left(ax_*+b\right)+1},$$

$$a_{31}=\frac{a^3x_*^4-6a^2x_*^2-4abx_*+a-b^2}{\left(ax_*^2+bx_*+1\right)^4},\ r_{00}=\frac{\left(\lambda_1+\lambda_2x_*\right)\left(x_*\left(ax_*+b\right)+1\right)^3}{a\left(3x_*\left(ax_*+b\right)-1\right)+b^2},$$

$$r_{10}=\frac{\lambda_2\left(x_*\left(ax_*+b\right)+1\right)^3}{a\left(3x_*\left(ax_*+b\right)-1\right)+b^2},\ r_{01}=-\lambda_1-\lambda_2x_*,$$

$$r_{20}=\frac{ax_*\left(3-ax_*^2\right)+b}{a\left(3x_*\left(ax_*+b\right)-1\right)+b^2},$$

$$r_{11}=-\lambda_2,\ r_{30}=\frac{a\left(ax_*^2\left(ax_*^2-6\right)-4bx_*+1\right)-b^2}{\left(x_*\left(ax_*+b\right)+1\right)\left(a\left(3x_*\left(ax_*+b\right)-1\right)+b^2\right)},$$

$$r_{21}=\frac{a^2x_*^3-3ax_*-b}{\left(ax_*^2+bx_*+1\right)^3},$$

$$r_{40} = \frac{-a^4x_*^5 + 10a^3x_*^3 + 5a^2x_*\left(2bx_* - 1\right) + ab\left(5bx_* - 2\right) + b^3}{\left(x_*\left(ax_* + b\right) + 1\right)^2\left(a\left(3x_*\left(ax_* + b\right) - 1\right) + b^2\right)},$$
$$r_{31} = \frac{-a^3x_*^4 + 6a^2x_*^2 + 4abx_* - a + b^2}{\left(ax_*^2 + bx_* + 1\right)^4}.$$

Next, we make the transformation

$$X = x,\quad Y = a_{00} + a_{10}x + a_{01}y + a_{20}x^2 + a_{11}xy + a_{30}x^3 + a_{21}x^2y + a_{40}x^4 + a_{31}x^3y + O(|x, y|^4).$$

Then system (36) becomes

$$\begin{aligned}\frac{dx}{dt} &= y,\\ \frac{dy}{dt} &= b_{00} + b_{10}x + b_{01}y + b_{20}x^2 + b_{11}xy + b_{02}y^2 + b_{30}x^3\\ &\quad + b_{21}x^2y + b_{12}xy^2 + b_{40}x^4 + b_{31}x^3y + b_{22}x^2y^2 + O(|x, y|^5),\end{aligned} \tag{37}$$

where

$$\begin{aligned}
b_{00} &= a_{01}r_{00} - a_{00}r_{01}, b_{10} = a_{11}r_{00} - a_{10}r_{01} + a_{01}r_{10} - a_{00}r_{11},\\
b_{01} &= a_{10} - \frac{a_{00}a_{11}}{a_{01}} + r_{01}, b_{20} = a_{21}r_{00} - a_{20}r_{01}\\
&\quad + a_{11}r_{10} - a_{10}r_{11} + a_{01}r_{20} - a_0r_{21},\\
b_{11} &= \frac{a_{00}a_{11}^2}{a_{01}^2} - \frac{a_{10}a_{11}}{a_{01}} + 2a_{20} - \frac{2a_{00}a_{21}}{a_{01}} + r_{11}, b_{02} = \frac{a_{11}}{a_{01}},\\
b_{30} &= a_{31}r_{00} - a_{30}r_{01} + a_{21}r_{10} - a_{20}r_{11} + a_{11}r_{20} - a_{10}r_{21} + a_{01}r_{30} - a_{00}r_{31},\\
b_{21} &= -\frac{a_{00}a_{11}^3}{a_{01}^3} + \frac{a_{10}a_{11}^2}{a_{01}^2}\\
&\quad + \frac{3a_{00}a_{21}a_{11}}{a_{01}^2} - \frac{a_{20}a_{11}}{a_{01}} + 3a_{30} - \frac{2a_{10}a_{21}}{a_{01}} - \frac{3a_{00}a_{31}}{a_{01}} + r_{21},\\
b_{12} &= \frac{2a_{21}}{a_{01}} - \frac{a_{11}^2}{a_{01}^2}, b_{40} = -a_{40}r_{01} + a_{31}r_{10} - a_{30}r_{11} + a_{21}r_{20}\\
&\quad - a_{20}r_{21} + a_{11}r_{30} - a_{10}r_{31} + a_{01}r_{40},\\
b_{31} &= \frac{a_{00}a_{11}^4}{a_{01}^4} - \frac{a_{10}a_{11}^3}{a_{01}^3} + \frac{a_{20}a_{11}^2}{a_{01}^2} - \frac{4a_{00}a_{21}a_{11}^2}{a_{01}^3} + \frac{3a_{10}a_{21}a_{11}}{a_{01}^2} + \frac{4a_{00}a_{31}a_{11}}{a_{01}^2}\\
&\quad - \frac{a_{30}a_{11}}{a_{01}} + \frac{2a_{00}a_{21}^2}{a_{01}^2} + 4a_{40} - \frac{2a_{20}a_{21}}{a_{01}} - \frac{3a_{10}a_{31}}{a_{01}} + r_{31},
\end{aligned}$$

$$b_{22} = \frac{a_{11}^3}{a_{01}^3} - \frac{3a_{21}a_{11}}{a_{01}^2} + \frac{3a_{31}}{a_{01}}.$$

Note that system (37) can be reduced to system (13) when $\lambda_1 = \lambda_2 = \lambda_3 = 0$.

Secondly, several steps are used to transform model (37) to the normal unfolding of the Bogdanov–Takens singularity of codimension 3. □

(I) Removing the y^2-term from system (37) We use the transformation $x = X + \frac{b_{02}}{2}X^2$, $y = Y + b_{02}XY$ to remove the y^2-term, then system (37) becomes

$$\begin{aligned}\frac{dx}{dt} &= y,\\ \frac{dy}{dt} &= c_{00} + c_{10}x + c_{01}y + c_{20}x^2 + c_{11}xy + c_{30}x^3\\ &\quad + c_{21}x^2y + c_{12}xy^2 + c_{40}x^4 + c_{31}x^3y + c_{22}x^2y^2 + O(|x, y|^5),\end{aligned} \tag{38}$$

where

$$\begin{aligned}&c_{00} = b_{00}, \quad c_{10} = b_{10} - b_{00}b_{02}, c_{01} = b_{01}, \quad c_{20} = b_{00}b_{02}^2 - \frac{b_{10}b_{02}}{2} + b_{20},\\ &c_{11} = b_{11}, c_{30} = -b_{00}b_{02}^3 + \frac{1}{2}b_{10}b_{02}^2 + b_{30}, c_{21} = \frac{b_{02}b_{11}}{2} + b_{21},\\ &c_{12} = 2b_{02}^2 + b_{12}, c_{40} = b_{00}b_{02}^4 - \frac{1}{2}b_{10}b_{02}^3 + \frac{1}{4}b_{20}b_{02}^2 + \frac{b_{30}b_{02}}{2} + b_{40},\\ &c_{31} = b_{02}b_{21} + b_{31}, c_{22} = -b_{02}^3 + \frac{3b_{12}b_{02}}{2} + b_{22}.\end{aligned}$$

We find that $c_{00} = c_{10} = c_{01} = c_{11} = 0$ when $\lambda_1 = \lambda_2 = \lambda_3 = 0$.

(II) Removing the xy^2-term from system (38) Let $x = X + \frac{c_{12}}{6}$, $y = Y + \frac{c_{12}}{2}X^2Y$. System (38) becomes the following, where xy^2 has been eliminated.

$$\begin{aligned}\frac{dx}{dt} &= y,\\ \frac{dy}{dt} &= d_{00} + d_{10}x + d_{01}y + d_{20}x^2 + d_{11}xy + d_{30}x^3\\ &\quad + d_{21}x^2y + d_{40}x^4 + d_{31}x^3y + d_{22}x^2y^2 + O(|x, y|^5),\end{aligned} \tag{39}$$

where

$$\begin{aligned}&d_{00} = c_{00}, \quad d_{10} = c_{10}, \quad d_{01} = c_{01},\\ &d_{20} = c_{20} - \frac{c_{00}c_{12}}{2}, \quad d_{11} = c_{11},\\ &d_{30} = c_{30} - \frac{c_{10}c_{12}}{3}, \quad d_{21} = c_{21},\\ &d_{40} = \frac{1}{4}c_{00}c_{12}^2 - \frac{c_{20}c_{12}}{6} + c_{40},\end{aligned}$$

$$d_{31} = \frac{c_{11}c_{12}}{6} + c_{31}, \qquad d_{22} = c_{22}.$$

Again we have that $d_{00} = d_{10} = d_{01} = d_{11} = 0$ when $\lambda_1 = \lambda_2 = \lambda_3 = 0$.

(III) Removing the x^2y^2-term from system (39) We assume $x = X + \frac{d_{22}}{12}X^4$, $y = Y + \frac{d_{22}}{3}X^2Y$. Model (39) becomes

$$\begin{aligned} \frac{dx}{dt} &= y, \\ \frac{dy}{dt} &= e_{00} + e_{10}x + e_{01}y + e_{20}x^2 + e_{11}xy + e_{30}x^3 \\ &\quad + e_{21}x^2y + e_{40}x^4 + e_{31}x^3y + O(|x, y|^5), \end{aligned} \tag{40}$$

where

$$\begin{aligned} &e_{00} = d_{00}, \quad e_{10} = d_{10}, \quad e_{01} = d_{01}, \quad e_{20} = d_{20}, \quad e_{11} = d_{11}, \\ &e_{30} = d_{30} - \frac{d_{00}d_{22}}{3}, \quad e_{21} = d_{21}, \quad e_{40} = d_{40} - \frac{d_{10}d_{22}}{4}, \quad e_{31} = d_{31}. \end{aligned}$$

It is clear that $e_{00} = e_{10} = e_{01} = e_{11} = 0$ when $\lambda_1 = \lambda_2 = \lambda_3 = 0$.

(IV) Removing the x^3-term and x^4-term from system (40) Note that

$$e_{20} = -\frac{x_*\left(ax_*\left(3 - ax_*^2\right) + b\right)}{\left(ax_*^2 + bx_* + 1\right)\left(a\left(3x_*\left(ax_* + b\right) - 1\right) + b^2\right)} + O(\lambda_1, \lambda_2, \lambda_3) \neq 0$$

for small λ. Let

$$\begin{aligned} x &= \frac{\left(15e_{30}^2 - 16e_{20}e_{40}\right)X^3}{80e_{20}^2} - \frac{e_{30}X^2}{4e_{20}} + X, \\ y &= Y, \\ t &= \tau\left(\frac{\left(45e_{30}^2 - 48e_{20}e_{40}\right)X^2}{80e_{20}^2} - \frac{e_{30}X}{2e_{20}} + 1\right). \end{aligned}$$

From model (40) we have

$$\begin{aligned} \frac{dx}{dt} &= y, \\ \frac{dy}{dt} &= f_{00} + f_{10}x + f_{01}y + f_{20}x^2 + f_{11}xy + f_{30}x^3 \\ &\quad + f_{21}x^2y + f_{40}x^4 + f_{31}x^3y + O(|x, y|^5), \end{aligned} \tag{41}$$

where

$$f_{00} = e_{00}, f_{10} = e_{10} - \frac{e_{00}e_{30}}{2e_{20}}, f_{01} = e_{01},$$

$$
\begin{aligned}
f_{20} &= \frac{9e_{00}e_{30}^2}{16e_{20}^2} - \frac{3e_{10}e_{30}}{4e_{20}} + e_{20} - \frac{3e_{00}e_{40}}{5e_{20}},\\
f_{11} &= e_{11} - \frac{e_{01}e_{30}}{2e_{20}},\ f_{30} = \frac{7e_{10}e_{30}^2}{8e_{20}^2} - \frac{4e_{10}e_{40}}{5e_{20}},\\
f_{21} &= \frac{9e_{01}e_{30}^2}{16e_{20}^2} - \frac{3e_{11}e_{30}}{4e_{20}} + e_{21} - \frac{3e_{01}e_{40}}{5e_{20}},\\
f_{40} &= \frac{e_{10}e_{30}e_{40}}{4e_{20}^2} - \frac{15e_{10}e_{30}^3}{64e_{20}^3},\\
f_{31} &= \frac{7e_{11}e_{30}^2}{8e_{20}^2} - \frac{e_{21}e_{30}}{e_{20}} + e_{31} - \frac{4e_{11}e_{40}}{5e_{20}}.
\end{aligned}
$$

We find that $f_{00} = f_{10} = f_{01} = f_{11} = f_{30} = f_{40} = 0$ when $\lambda_1 = \lambda_2 = \lambda_3 = 0$.

(V) Removing the x^2y-term from system (41) Since $f_{20} = \frac{x_*(a^2x_*^3 - 3ax_* - b)}{(ax_*^2 + bx_* + 1)(3a^2x_*^2 + 3abx_* - a + b^2)} + O(\lambda_1, \lambda_2, \lambda_3) \neq 0$ for small λ, we choose the following transformation

$$
x = X,\quad y = \frac{f_{21}^2 Y^3}{36 f_{20}^2} + \frac{f_{21} Y^2}{3 f_{20}} + Y,\quad \tau = t\left(\frac{f_{21}^2 Y^2}{36 f_{20}^2} + \frac{f_{21} Y}{3 f_{20}} + 1\right),
$$

and get a new system of system (41) as follows (we still denote X, Y, τ by x, y, t, respectively)

$$
\begin{aligned}
\frac{dx}{dt} &= y,\\
\frac{dy}{dt} &= g_{00} + g_{10}x + g_{01}y + g_{20}x^2 + g_{11}xy + g_{31}x^3y + R_1(x, y, \lambda),
\end{aligned}
\tag{42}
$$

where

$$
\begin{aligned}
g_{00} &= f_{00},\ g_{10} = f_{10},\ g_{01} = f_{01} - \frac{f_0 f_{21}}{f_{20}},\\
g_{20} &= f_{20},\ g_{11} = f_{11} - \frac{f_{10} f_{21}}{f_{20}},\ g_{31} = f_{31} - \frac{f_{21} f_{30}}{f_{20}}.
\end{aligned}
$$

We find that $g_{00} = g_{10} = g_{01} = g_{11} = 0$ when $\lambda_1 = \lambda_2 = \lambda_3 = 0$. $R_1(x, y, \lambda)$ has the property in (4.6) of Arsie at al. [21] which is one of the conditions undergoing a Bogdanov–Takens bifurcation of codimension 3 (see, also, Lamontagne et al. [44], and Chow et al. [47]).

(VI) Changing g_{20} and g_{11} to 1 in system (42) We notice that

$$
\begin{aligned}
g_{20} &= \frac{x_*\left(a^2x_*^3 - 3ax_* - b\right)}{\left(ax_*^2 + bx_* + 1\right)\left(3a^2x_*^2 + 3abx_* - a + b^2\right)} + O(\lambda) \neq 0,\\
g_{31} &= \frac{1}{\left(ax_*^2 + bx_* + 1\right)\left(3a^2x_*^2 + 3abx_* - a + b^2\right)\left(-a^2x_*^3 + 3ax_* + b\right)}\\
&\quad \times (12a^5x_*^6 + 12a^4bx_*^5 - 3b^4 - 64a^4x_*^4 + 4a^3b^2x_*^4\\
&\quad - 96a^3bx_*^3 + 36a^3x_*^2 - 66a^2b^2x_*^2 + 28a^2bx_*\\
&\quad - 22ab^3x_* + 6ab^2) + O(\lambda) \neq 0.
\end{aligned}
$$

for small λ. By making the following transformation

$$
x = \sqrt[5]{g_{20}}g_{31}^{-\frac{2}{5}}X, \quad y = g_{20}^{4/5}g_{31}^{-\frac{3}{5}}Y, \quad t = g_{20}^{-\frac{3}{5}}\sqrt[5]{g_{31}}\tau,
$$

we can transform system (42) into (we still denote X, Y, τ by x, y, t respectively)

$$
\begin{aligned}
\frac{dx}{dt} &= y,\\
\frac{dy}{dt} &= h_{00} + h_{10}x + h_{01}y + x^2 + h_{11}xy + x^3y + R_2(x, y, \lambda),
\end{aligned}
\tag{43}
$$

where

$$
h_{00} = \frac{g_0g_{31}^{4/5}}{g_{20}^{7/5}}, \quad h_{10} = \frac{g_{10}g_{31}^{2/5}}{g_{20}^{6/5}}, \quad h_{01} = \frac{g_1\sqrt[5]{g_{31}}}{g_{20}^{3/5}}, \quad h_{11} = \frac{g_{11}}{g_{20}^{2/5}\sqrt[5]{g_{31}}}.
$$

Note that $h_{00} = h_{10} = h_{01} = h_{11} = 0$ when $\lambda_1 = \lambda_2 = \lambda_3 = 0$, and $R_2(x, y, \lambda)$ has the same property as $R_1(x, y, \lambda)$.

(VII) Removing x-term from system (43) Let $x = X - \frac{h_{10}}{2}, y = Y$. System (43) becomes (we still denote X, Y by x, y, respectively)

$$
\begin{aligned}
\frac{dx}{dt} &= y,\\
\frac{dy}{dt} &= \nu_1 + \nu_2y + \nu_3xy + x^2 + x^3y + R_3(x, y, \lambda),
\end{aligned}
\tag{44}
$$

where $\nu_1 = h_0 - \frac{h_{10}^2}{4}$, $\nu_2 = -\frac{h_{10}^3}{8} - \frac{h_{11}h_{10}}{2} + h_1$, $\nu_3 = \frac{3h_{10}^2}{4} + h_{11}$, and $R_3(x, y, \lambda)$ has the same property as $R_1(x, y, \lambda)$.

Next, with the help of *Mathematica*, we have

$$\begin{aligned}
&\left|\frac{\partial(\nu_1,\nu_2,\nu_3)}{\partial(\lambda_1,\lambda_2,\lambda_3)}\right|_{\lambda=0}\\
&=\frac{3x_*\left(x_*\left(ax_*+b\right)+1\right)^3}{4\,2^{4/5}\left(ax_*\left(3-ax_*^2\right)+b\right)^2\left(\frac{x_*^3\left(ax_*\left(ax_*^2-3\right)-b\right)}{\left(x_*\left(ax_*+b\right)+1\right)^2\left(x_*\left(3ax_*+b\right)-1\right)}\right)^{7/5}}\\
&\times\left(x_*\left(b^2x_*\left(5ax_*^2-3\right)+b\left(ax_*^2\left(7ax_*^2-10\right)-1\right)\right.\right.\\
&\left.\left.+ax_*\left(ax_*^2\left(7ax_*^2-19\right)+5\right)+b^3x_*^2\right)-1\right)\\
&\times\left(-\frac{R}{x_*\left(x_*\left(ax_*+b\right)+1\right)^2\left(x_*\left(3ax_*+b\right)-1\right)\left(ax_*\left(3-ax_*^2\right)+b\right)}\right)^{4/5},
\end{aligned}$$

where

$$\begin{aligned}
R=&-12a^5x_*^9-16a^4bx_*^8+91a^3bx_*^6+x_*^4\left(23a^2b+25ab^3\right)\\
&+x_*^3\left(-58a^2+20ab^2+3b^4\right)\\
&+x_*^7\left(34a^4-4a^3b^2\right)+x_*^5\left(46a^3+67a^2b^2\right)\\
&+x_*^2\left(3b^3-19ab\right)+x_*\left(6a-3b^2\right)+b.
\end{aligned}$$

Thus, system (4) goes through a codimension-3 Bogdanov–Taken bifurcation.

3.3 Hopf Bifurcation

In this subsection, we study the Hopf bifurcation of system (4) near the equilibrium $E_\alpha(x_\alpha, y_\alpha)$ to find the existence condition of the limit cycle. As we know, there are several methods to investigate the existence of degenerate Hopf bifurcation, for example, Poincaré normal form [48], averaging method [47], successive function method [49], Lyapunov-Schmidt reduction [50].

Theorem 3.3 *No limit cycles can be found for system* (4) *if (a)* $bd+\eta-1>0$ *or (b)* $bd+\eta-1<0$ *and* $h(x_2)>0$*; (c).* $G'(x)>0$ *for all* $x\in(s_1,\beta)$*, where* $s_1=max\{0,A\}$.

Proof There is no positive equilibrium for system (4) when condition (a) or (b) holds. Thus system (4) has no limit cycles. For condition (c), we make the following transformation

$$\hat{x}=\ln x,\quad \hat{y}=\ln y,\quad \tau=\frac{t}{ax^2+bx+1},$$

then we have

$$\frac{d\hat{x}}{d\tau} = G(e^{\hat{x}}) - e^{\hat{y}}, \quad \frac{d\hat{y}}{d\tau} = -h(e^{\hat{x}}),$$

where $h(\cdot)$ is given in Eq. (5). Since $G'(x)$ is positive for any $x \in (s_1, \beta)$, we obtain

$$\nabla \cdot \langle G(e^{\hat{x}}) - e^{\hat{y}}, -h(e^{\hat{x}}) \rangle = \frac{d}{d\hat{x}}(G(e^{\hat{x}}) - e^{\hat{y}}) + \frac{d}{d\hat{y}}(-h(e^{\hat{x}})) = e^{\hat{x}} G'(e^{\hat{x}}) > 0.$$

Using Dulac's criteria, we know that system (4) has no limit cycles in the positive cone. □

Theorem 3.4 *If $A \leq 0$, $\alpha < \mathcal{K} < \beta$, and $G'(\alpha) > 0$, then system (4) has a limit cycle.*

Proof It is easy to know that system (4) has three equilibria E_0, $E_{\mathcal{K}}$ and E_α if $A \leq 0$, $G'(\alpha) > 0$, and $\alpha < \mathcal{K} < \beta$. On the coordinate axes, there are stable manifolds of two saddles E_0 and $E_{\mathcal{K}}$. In particular, all orbits in the positive cone will remain in the compact set, bounded by x-axis, y-axis and $x + y = M$. E_α is an unstable focus or node. Thus, there exists a limit cycle surrounding the equilibrium E_α by Poincare-Bendixson Theorem.

Now, we turn to compute the Lyapunov coefficient of the Hopf bifurcation point. In order to simplify the computation as used in Perko [43], we let

$$\bar{x} = \frac{x}{x_\alpha}, \quad \bar{y} = \frac{y}{y_\alpha}, \quad \tau = x_\alpha^2 t \tag{45}$$

and change model (4) to (use t instead of τ)

$$\begin{aligned} \frac{d\bar{x}}{dt} &= \frac{1}{x_\alpha^3}\left(x_\alpha \bar{x}\,(x_\alpha \bar{x} - A)\,(\mathcal{K} - x_\alpha \bar{x}) - \frac{y_\alpha\,(x_\alpha \bar{x})\,\bar{y}}{a\,(x_\alpha \bar{x})^{\,2} + b x_\alpha \bar{x} + 1} \right), \\ \frac{d\bar{y}}{dt} &= \frac{1}{x_\alpha^2 y_\alpha}\left(y_\alpha \bar{y}\left(\frac{x_\alpha \bar{x}}{a\,(x_\alpha \bar{x})^{\,2} + b x_\alpha \bar{x} + 1} - \eta x_\alpha \bar{x} - d \right) \right). \end{aligned} \tag{46}$$

Substituting the following parameter scaling

$$a = \frac{\bar{a}}{x_\alpha^2}, \quad b = \frac{\bar{b}}{x_\alpha}, \quad \mathcal{K} = x_\alpha \bar{\mathcal{K}}, \quad A = x_\alpha \bar{A}, \quad d = x_\alpha \bar{d}, \quad \eta = \bar{\eta}, \quad q = \frac{1}{x_\alpha},$$

into system (46), with the help of (3) to eliminate y_α and drop the bars, we have

$$\begin{aligned} \frac{dx}{dt} &= x\left(\frac{(A-1)(\mathcal{K}-1)y(a+b+1)}{ax^2 + bx + 1} + (A - x)(x - \mathcal{K}) \right), \\ \frac{dy}{dt} &= qy\left(\frac{x}{ax^2 + bx + 1} - d - \eta x \right). \end{aligned} \tag{47}$$

Since system (47) has an equilibrium $\bar{E_\alpha}(1,1)$ (i.e., $E_\alpha(x_\alpha, y_\alpha)$) of system (4), then

$$d = \frac{-(a+b+1)\eta + 1}{a+b+1},$$

which is substituted into system (47) and we obtain the following system

$$\begin{aligned} \frac{dx}{dt} &= x\left(\frac{(A-1)(\mathcal{K}-1)y(a+b+1)}{ax^2+bx+1} + (A-x)(x-\mathcal{K})\right), \\ \frac{dy}{dt} &= qy\left(\frac{x}{ax^2+bx+1} - \frac{-a\eta - b\eta - \eta + 1}{a+b+1} - \eta x\right), \end{aligned} \tag{48}$$

where

$$\begin{aligned} &a, c, \mathcal{K} > 0, -\mathcal{K} < A < \mathcal{K}, d > 0 \to 0 < \eta < \frac{1}{1+a+b}, \\ &b > -2\sqrt{a}, 0 < x_\alpha < 1 \to q > 1. \end{aligned} \tag{49}$$

It is obvious to see that system (48) has the same qualitative property as system (4) because transformation (45) is a linear sign-reserving transformation.
Next, we investigate the dynamics of system (48) in $R_2^+ = \{(x, y)|x \geq 0, y \geq 0\}$. In what follows, the Hopf bifurcation around new equilibrium $\tilde{E_\alpha}(1,1)$ of system (48) is studied, which is corresponding to the Hopf bifurcation around $E_\alpha(x_\alpha, y_\alpha)$) in model (4). □

Theorem 3.5 *If* (49) *and* (52) *hold, then system* (48) *has an equilibrium* $\tilde{E_\alpha}(1,1)$. *Moreover,*

(i) *if* $\mathcal{K} < \mathcal{K}^*$, *then* $\tilde{E_\alpha}(1,1)$ *is an unstable hyperbolic node or focus;*
(ii) *if* $\mathcal{K} > \mathcal{K}^*$, *then* $\tilde{E_\alpha}(1,1)$ *is a locally asymptotically stable hyperbolic node or focus;*
(iii) *if* $\mathcal{K} = \mathcal{K}^*$, *then* $\tilde{E_\alpha}(1,1)$ *is a weak focus or center.*

Proof Firstly, we define the Jacobian matrix $J(\tilde{E_\alpha}(1,1))$ of system (48) at $\tilde{E_\alpha}(1,1)$ is as follows:

$$J(\tilde{E_\alpha}(1,1)) = \begin{pmatrix} \frac{2bA - b\mathcal{K}A + A - 3b + 2b\mathcal{K} + \mathcal{K} + a(3\mathcal{K} + A(3-2\mathcal{K}) - 4) - 2}{a+b+1} & (A-1)(\mathcal{K}-1) \\ q\left(\frac{1-a}{(a+b+1)^2} - \eta\right) & 0 \end{pmatrix}. \tag{50}$$

Its determinant and trace are

$$\det(J(\tilde{E_\alpha}(1,1))) = \frac{(A-1)(\mathcal{K}-1)q\left(\eta(a+b+1)^2 + a - 1\right)}{(a+b+1)^2},$$

and

$$\begin{aligned}&\mathrm{tr}(J(\tilde{E_\alpha}(1,1)))\\&=\frac{a(A(3-2\mathcal{K})+3\mathcal{K}-4)-Ab\mathcal{K}+2Ab+A+2b\mathcal{K}-3b+\mathcal{K}-2}{a+b+1}.\end{aligned}$$

From $y_\alpha = (x_\alpha - A)(\mathcal{K} - x_\alpha)(ax_\alpha^2 + bx_\alpha + 1) = (x_\alpha - \bar{A}x_\alpha)(\bar{\mathcal{K}}x_\alpha - x_\alpha)(ax_\alpha^2 + bx_\alpha + 1) = x_\alpha^2(1-\bar{A})(\bar{\mathcal{K}}-1)(ax_\alpha^2 + bx_\alpha + 1) > 0$, we have (drop bars)

$$(1-A)(\mathcal{K}-1) > 0 \tag{51}$$

and $\det(J(\tilde{E_\alpha}(1,1))) > 0$ if

$$\eta(a+b+1)^2 + a - 1 < 0, \tag{52}$$

and $\mathrm{tr}(J(\tilde{E_\alpha}(1,1))) = 0$ (> 0 or < 0) if $\mathcal{K} = \mathcal{K}^*$ ($\mathcal{K} < \mathcal{K}^*$ or $\mathcal{K} > \mathcal{K}^*$), where

$$\begin{aligned}\mathcal{K}^* &= \frac{a(3A-4)+2Ab+A-3b-2}{a(2A-3)+(A-2)b-1}\\&= 1+\frac{(1+a+b)(A-1)}{-1+a(-3+2A)+(-2+A)b}.\end{aligned} \tag{53}$$

When condition (49) holds, we have

$$-1+a(-3+2A)+(-2+A)b < 0, \quad \mathcal{K} > 1, \quad A < 1. \tag{54}$$

It is easy to obtain

$$\frac{d}{d\mathcal{K}}(\mathrm{tr}(J(\tilde{E_\alpha}(1,1))))|_{\mathcal{K}=\mathcal{K}^*} = \frac{1-a(2A-3)-(A-2)b}{a+b+1} > 0.$$

Next, we focus on case (iii) in Theorem 3.3 and study the existence of Hopf bifurcation around $\tilde{E_\alpha}(1,1)$ of system (48), which is equal to the existence of Hopf bifurcation around $E_\alpha(x_\alpha, y_\alpha)$ of system (4). We show the stability of the Hopf bifurcation and periodic orbits near the positive equilibrium $\tilde{E_\alpha}(1,1)$ of model (48) by computing the Lyapunov coefficient.

Setting $X = x - 1$, $Y = y - 1$, and $\mathcal{K} = \mathcal{K}^*$, we rewrite system (48) as follows

$$\begin{aligned}\frac{dx}{dt} &= a_{01}y + a_{20}x^2 + a_{11}xy + a_{30}x^3 + a_{21}x^2y,\\\frac{dy}{dt} &= b_{10}x + b_{20}x^2 + b_{11}xy + b_{30}x^3 + b_{21}x^2y,\end{aligned} \tag{55}$$

where

$$
\begin{aligned}
a_{01} &= \frac{aA^2 - 2aA + a + A^2b + A^2 - 2Ab - 2A + b + 1}{2aA - 3a + Ab - 2b - 1},\\
a_{20} &= \frac{(A-1)^2\left(3a^2 + 3ab - a + b^2\right)}{(a+b+1)(2aA - 3a + Ab - 2b - 1)} - 1,\\
a_{11} &= \frac{-aA^2 + 2aA - a + A^2 - 2A + 1}{2aA - 3a + Ab - 2b - 1},\\
a_{30} &= -\frac{(a-1)^2(A-1)}{(a+b+1)^2} + \frac{a(A-2) + A}{a+b+1} + \frac{1 - a(A-2)^2}{a(2A-3) + (A-2)b - 1} - 1,\\
a_{21} &= \frac{a^2A^2 - 2a^2A + a^2 - 3aA^2 + 6aA - 3a - A^2b + 2Ab - b}{(a+b+1)(2aA - 3a + Ab - 2b - 1)},\\
b_{10} &= -\frac{aq}{(a+b+1)^2} + \frac{q}{(a+b+1)^2} - \eta q,\\
b_{20} &= \frac{q\left(a^2 - 3a - b\right)}{(a+b+1)^3}, b_{11} = -\frac{aq}{(a+b+1)^2} + \frac{q}{(a+b+1)^2} - \eta q,\\
b_{30} &= -\frac{q\left(a^3 - 6a^2 - 4ab + a - b^2\right)}{(a+b+1)^4}, b_{21} = \frac{q\left(a^2 - 3a - b\right)}{(a+b+1)^3}.
\end{aligned}
$$

Using the transformation

$$
X = x, \quad Y = \sqrt{-\frac{a_1}{b_{10}}}y, \quad \tau = -b_{10}\sqrt{-\frac{a_1}{b_{10}}}t,
$$

we transform system (55) into

$$
\begin{aligned}
\frac{dx}{dt} &= y + \frac{a_{20}\sqrt{-\frac{a_{01}}{b_{10}}}}{a_{01}}x^2 + \frac{a_{11}}{a_{01}}xy + \frac{a_{30}\sqrt{-\frac{a_{01}}{b_{10}}}}{a_{01}}x^3 + \frac{a_{21}}{a_{01}}x^2y,\\
\frac{dy}{dt} &= -x + \left(-\frac{b_{20}}{b_{10}}\right)x^2 + \frac{b_{11}\sqrt{-\frac{a_{01}}{b_{10}}}}{a_{01}}xy + \left(-\frac{b_{30}}{b_{10}}\right)x^3 + \frac{b_{21}\sqrt{-\frac{a_{01}}{b_{10}}}}{a_{01}}x^2y.
\end{aligned}
\tag{56}
$$

By virtue of the formula used in Zhang et al. [51] and calculation by *Matlab* and *Mathematica*, we have the first Lyapunov coefficient as follows

$$
\sigma_1 = \frac{\sqrt{\frac{(A-1)^2(a+b+1)^3}{q(a(2A-3)+(A-2)b-1)\left(\eta(a+b+1)^2+a-1\right)}}\sigma_{11}}{8(A-1)^2(a+b+1)^2\left(\eta(a+b+1)^2 + a - 1\right)},
$$

where

$$
\begin{aligned}
\rho_1 &= -2A^2b^2 + 9Ab^2 + 2Ab - 12b^2 - 9b - 2,\\
\rho_2 &= -9A^2b + 2A^2 - 3Ab^2 + 36Ab + 6b^2 - 37b - 12,
\end{aligned}
$$

$$
\begin{aligned}
\rho_3 &= 3A^2b - 12A^2 - 18Ab + 40A + 24b - 30,\\
\rho_4 &= 6A^2 - 24A + 24,\\
\rho_5 &= 2A^2b^3 + 2A^2b^2 - 3Ab^4 - 12Ab^3 - 11Ab^2\\
&\quad - 2Ab + 6b^4 + 21b^3 + 24b^2 + 11b + 2,\\
\rho_6 &= A^2b^3 + 12A^2b^2 + 7A^2b - 2A^2 - 18Ab^3 - 58Ab^2\\
&\quad - 36Ab + 30b^3 + 82b^2 + 62b + 12,\\
\rho_7 &= 4A^2b^2 + 26A^2b + 12A^2 - 39Ab^2 - 98Ab - 40A + 56b^2 + 111b + 46,\\
\rho_8 &= 3A^2b + 14A^2 - 32Ab - 48A + 44b + 48,\\
\rho_9 &= 12 - 8A,
\end{aligned}
$$

and

$$\sigma_{11} = \rho_1 + \rho_2 a + \rho_3 a^2 + \rho_4 a^3 + (\rho_5 + \rho_6 a + \rho_7 a^2 + \rho_8 a^3 + \rho_9 a^4)\eta. \quad (57)$$

From conditions (52) and (54), we find the sign of the σ_1 is opposite to that of σ_{11}. Thus, we obtain the following results. □

Theorem 3.6 *Suppose $\mathcal{K} = \mathcal{K}^*$ and conditions (49), (51), (52) and (54) are satisfied.*

(i) *when $\sigma_{11} > 0$, we have a stable weak focus $\tilde{E}(1, 1)$ with multiplicity one and a stable limit cycle bifurcating from $\tilde{E}(1, 1)$, i.e., system (48) undergoes a supercritical Hopf bifurcation;*

(ii) *when $\sigma_{11} < 0$, we have an unstable weak focus $\tilde{E}(1, 1)$ with multiplicity one and an unstable limit cycle bifurcating from $\tilde{E}(1, 1)$, i.e., system (48) undergoes a subcritical Hopf bifurcation;*

(iii) *when $\sigma_{11} = 0$, we have a weak focus $\tilde{E}(1, 1)$ with multiplicity of at least two and model (48) has a degenerate Hopf bifurcation of at least codimension 2.*

Next, we focus on case (iii) in Theorem 3.4. We find $\sigma_{11} = 0$ if

$$\eta = \eta^* = \frac{\rho_1 + \rho_2 a + \rho_3 a^2 + \rho_4 a^3}{-(\rho_5 + \rho_6 a + \rho_7 a^2 + \rho_8 a^3 + \rho_9 a^4)}. \quad (58)$$

From case (iii) of Theorem 3.4, it is easy to know that system (48) could undergo a degenerate Hopf bifurcation which is a codimension-2 Hopf bifurcation as $\mathcal{K} = \mathcal{K}^*$ and $\eta = \eta^*$. Using the formal series method in Freedman and Wolkowicz [10], with the help of *Mathematica* and *Matlab* software, the second Lyapunov coefficient is obtained as follows

$$\sigma_2 = \frac{-\sigma_{22}}{32\sqrt{2}(-1 + a(-3 + 2A) + (-2 + A)b)m_1 q\sqrt{\frac{-m_3}{m_2}}},$$

where

$$
\begin{aligned}
m_1 &= (a+b+1)^3(b-(a-3)a)^2(1+a^2(6+A(-8+3A))\\
&\quad + b(3-A+(3+(-3+A)A)b)\\
&\quad + a(3-A^2+(8+3(-3+A)A)b))^2 > 0,\\
m_2 &= (A^2\left(3a^2+3ab-a+b^2\right)+A\left(-8a^2-9ab-3b^2-b\right)\\
&\quad + a(6a+8b+3)+3b^2+3b+1)\\
&\quad \times ((a-3)a-b)(a(2A-3)+(A-2)b-1)q \neq 0,\\
m_3 &= (A-1)^2(a+b+1)^3(-8a^3A+12a^3+3a^2A^2b+14a^2A^2\\
&\quad - 24a^2Ab-40a^2A+32a^2b\\
&\quad + aA^2b^2+9aA^2b-2aA^2-15aAb^2-34aAb+24ab^2\\
&\quad + 43ab+10a+2A^2b^2-3Ab^3\\
&\quad - 2Ab+6b^3+15b^2+9b+2+36a^2-9Ab^2) \neq 0,\\
\sigma_{22} &= -(m_4+m_5q).
\end{aligned}
$$

Note that m_4 and m_5 are too complicated and are omitted for simplicity. For example, we take $a = 0.0015$, $b = -0.035$, $A = -5$, and according to conditions (49), (52) and (54), we have $\mathcal{K} = 8.48741$, $\eta = 1.0344$. Then $m_4 = 0.0041025$, $m_5 = -0.0000206483$, and $\sigma_{22} = -(m_4 + m_5q) = -(0.0041025 - 0.0000206483 \times 198.684) = -1.31628 \times 10^{-8} < 0$, i.e., system (48) has two coexistent limit cycles. Since $-1 + a(2A-3) + (A-2)b < 0$ and $m_1 > 0$, the sign of σ_2 is determined by σ_{22}.

Then we obtain the following results. □

Theorem 3.7 *Suppose $\mathcal{K} = \mathcal{K}^*$, $\eta = \eta^*$ and conditions (49), (51), (52) and (54) are satisfied.*

(i) *if $\sigma_{22} > 0$, then we have an unstable weak focus $\tilde{E}(1,1)$ with multiplicity two. Model (48) has a codimension-2 degenerate Hopf bifurcation, i.e., two limit cycles (the inner one and the outer one are, respectively, stable and unstable) originating from $\tilde{E}(1,1)$.*

(ii) *if $\sigma_{22} < 0$, then we have a stable weak focus $\tilde{E}(1,1)$ with multiplicity two. Model (48) has a codimension-2 degenerate Hopf bifurcation, i.e., two limit cycles (the inner one and the outer one are, respectively, unstable and stable) originating from $\tilde{E}(1,1)$.*

(iii) *if $\sigma_{22} = 0$, then we have a weak focus $\tilde{E}(1,1)$ with multiplicity of at least three. Model (48) may have a degenerate Hopf bifurcation of codimension ≥ 3, i.e., three limit cycles are originating from $\tilde{E}(1,1)$.*

Next, we focus on case (iii) of Theorem 3.5. When $\sigma_2 = 0$ equals to $\sigma_{22} = 0$, i.e.,

$$
q = \frac{-m_4}{m_5}, \tag{59}
$$

system (48) may have degenerate Hopf bifurcation of codimension ≥ 3.

From case (iii) of Theorem 3.5, we see that system (48) may undergo a degenerate Hopf bifurcation of codimension 2 as $\mathcal{K} = \mathcal{K}^*$, $\eta = \eta^*$ and $q = q^*$. By virtue of the formal series method used in Freedman and Wolkowicz [10] and with the help of *Mathematica* and *Matlab* software, the following third Lyapunov coefficient is obtained

$$\sigma_3 = \frac{\frac{1}{663552}\sigma_{33}}{(1-a(-3+2A)-(-2+A)b)^3\sqrt{\frac{(A-1)^2(a+b+1)^3}{q(a(2A-3)+(A-2)b-1)(a^2\eta+a(2(b+1)\eta+1)+(b+1)^2\eta-1)}}N_0},$$

where $N_0 = (-1+A)^4(1+a+b)^6q^6(-1+a^2\eta+(1+b)^2\eta+a(1+2(1+b)\eta))^6 > 0$, $\sigma_{33} = -(N_1 + N_2A^2 + N_3A^4)$. It is noted that the expressions of N_i, $(i = 1, 2, 3)$ are tedious, for simplicity, we omit them here. Since $1 - a(2A - 3) - (A - 2)b > 0$ and $N_0 > 0$, the sign of σ_3 is determined by σ_{33}. Then we get the following results.

Theorem 3.8 *Assume $\mathcal{K} = \mathcal{K}^*$, $\eta = \eta^*$, $q = q^*$ and conditions (49), (51), (52) and (54) are satisfied, we have*

(i) *if $\sigma_{33} > 0$, then we have an unstable weak focus $\tilde{E}(1, 1)$ with multiplicity three. Model (48) undergoes a codimension-3 degenerate Hopf bifurcation, i.e., three limit cycles are originating from $\tilde{E}(1, 1)$;*

(ii) *if $\sigma_{33} < 0$, then we have a stable weak focus $\tilde{E}(1, 1)$ with multiplicity three. Model (48) undergoes a codimension-3 degenerate Hopf bifurcation, i.e., three limit cycles are originating from $\tilde{E}(1, 1)$;*

(iii) *if $\sigma_{33} = 0$, then we have a weak focus $\tilde{E}(1, 1)$ with multiplicity ≥ 4. Model (48) may have degenerate Hopf bifurcation of codimension ≥ 4, i.e., four limit cycles are originating from $\tilde{E}(1, 1)$.*

4 Cusp of Limit Cycle with Codimension 2

In this subsection, we revisit the periodic normal form on the center manifold according to Witte et al. [52] and Iooss [53].

Rewrite a general ODE system at $\dot{u} = F(u)$, and assume that a limit cycle γ satisfies $u(0) = u(T)$, where $T > 0$ is the minimum period. Expand $F(u_0(t) + v)$ by using the Taylor expansion as follows:

$$\begin{aligned} F(u_0(t)+v(t)) = {} & F(u_0(t)) + A(t)v(t) + \frac{1}{2!}B(t; v_1(t), v_2(t)) \\ & + \frac{1}{3!}C(t; v_1(t), v_2(t), v_3(t)) \\ & + \frac{1}{4!}D(t; v_1(t), v_2(t), v_3(t), v_4(t)) \\ & + \frac{1}{5!}E(t; v_1(t), v_2(t), v_3(t), v_4(t), v_5(t)) + O(||v||^6), \quad (60) \end{aligned}$$

where

$$\begin{aligned} A(t)v &= F_u(u_0(t))v, \\ B(t; v_1(t), v_2(t)) &= F_{uu}[v_1, v_2], \\ C(t; v_1(t), v_2(t), v_3(t)) &= F_{uuu}[v_1, v_2, v_3], \\ D(t; v_1(t), v_2(t), v_3(t), v_4(t)) &= F_{uuuu}[v_1, v_2, v_3, v_4], \\ E(t; v_1(t), v_2(t), v_3(t), v_4(t), v_5(t)) &= F_{uuuuu}[v_1, v_2, v_3, v_4, v_5]. \end{aligned} \tag{61}$$

Define the initial-value problem for the fundamental matrix solution $Y(t)$ as follows

$$\frac{dY}{dt} = A(t)Y, \quad y(0) = I_n, \tag{62}$$

where I_n denotes the $n \times n$ identity matrix. We call The eigenvalues of the monodromy matrix $M = Y(T)$ as (Floquet) multipliers of the limit cycle. The multipliers with $|\mu| = 1$ denote the critical multipliers. A trivial critical multiplier $\mu_n = 1$ always exists. The total number of critical multipliers (counting multiplicity) is denoted by n_c, and assume that the limit cycle is nonhyperbolic, i.e., $n_c = 2$. Therefore, there is an invariant n_c-dimensional critical center manifold $W^c(\tau) \subset R^n$ in the neighborhood of τ.

Note that, there is a two-dimensional critical center manifold $W^c(\tau)$ at the cusp point of limit cycles (CPL) bifurcation, which can be parameterized locally by (τ, ξ) as

$$u = u_0(\tau) + \xi v(\tau) + H(\tau, \xi), \tau \in [0, T], \xi \in R, \tag{63}$$

where

$$H(\tau, \xi) = \frac{1}{2}h_2(\tau)\xi^2 + \frac{1}{6}h_2(\tau)\xi^3 + O(\xi^4), \tag{64}$$

satisfying $H(T, \xi) = H(0, \xi)$, $h_2(0) = h_2(T)$ and $h_3(0) = h_3(T)$.

The normal form of codimension-2 cusp of limit cycle can be defined as follows:

$$\dot{\xi} = c\xi^3, \quad \xi \in R, \tag{65}$$

where

$$\begin{aligned} c = \frac{1}{6}\int_0^T &< \varphi^*, -6\alpha_1 A(\tau)v + 3A(\tau)h_2 + 3B(\tau; v_1, v_2) \\ &+ 6A(\tau)v + 3B(\tau; v_1, h_2, v_2) + C(\tau; v_1, v_2, v_3) > d\tau, \end{aligned} \tag{66}$$

v and φ^* are the generalized eigenfunction and a nontrivial solution of the adjoint eigenvalue problem, respectively, defined by

$$\begin{cases} \dot{v} - A(\tau)v - F(u_0) = 0, \tau \in [0, T], \\ v(T) - v(0) = 0, \\ \int_0^T < v, u_0 > d\tau = 0, \end{cases} \quad \begin{cases} \dot{\varphi^*} - A^T(\tau)\varphi^* = 0, \tau \in [0, T], \\ \varphi^*(T) - \varphi^*(0) = 0. \\ \int_0^T < \varphi^*, v > d\tau = 1, \end{cases}$$

and h_2 is a unique solution of

$$\begin{cases} \dot{h_2} - A^T(\tau)h_2 - B(\tau; v, v) - 2Av - 2F(u_0) + 2\alpha_1 F(u_0) = 0, \tau \in [0, T], \\ h_2(T) - h_2(0) = 0, \\ \int_0^T < v^*, h_2 > d\tau = 1. \end{cases}$$

5 Numerical Simulations

In this section, we choose parameter values to illustrate the theoretical results by using numerical simulations with the aid of ODE software Matlab and AUTO [54].

We consider the role of the strong Allee effect by setting

$$\mathcal{K} = 20, A = 2, a = 0.004905, b = -0.10891, d = 24.28, \eta = 0.005, \quad (67)$$

which have been used in Arsie et al. [21].

5.1 $\mathcal{K}$ and η as the Bifurcation Parameters

The carrying capacity of the prey ($\mathcal{K}$) is first used as the bifurcation parameter. There are four boundary equilibria $E_0(0, 0)$, $E_A(2, 0)$, $E_{\mathcal{K}1}(9.81763, 0)$, $E_{\mathcal{K}2}(2.07305 \times 10^1, 0)$. All the boundary equilibria are transcritical bifurcation points, and there is one subcritical Hopf bifurcation point $HB(9.81763, 3.26253 \times 10^1)$ as $\mathcal{K} = 2.01595 \times 10^1$. The limit cycle branch bifurcating the Hopf point HB has one saddle-node $SN(1.37493 \times 10^1, 3.81486 \times 10^1)$ as $\mathcal{K} = 1.99229 \times 10^1$, $period = 1.38636 \times 10^{-1}$. A family of limit cycles is approaching an unstable homoclinic cycle. The transition of stability of equilibria is given in Fig. 2.

Next, the carrying capacity of the prey ($\mathcal{K}$) and the intensity of anti-predator behavior (η) are used as the bifurcation parameters. We obtain two-parameter bifurcation diagram including Hopf bifurcation curve H (purple) saddle-node bifurcation curve SN (green), homoclinic bifurcation curve Hom (red), and saddle-node bifurcation curve of limit cycle SNL (blue). We have one Bogdanov–Takens bifurcation point $BT(1.35362 \times 10^1, 3.42613 \times 10^1)$ as $\mathcal{K} = 2.05323 \times 10^1$, $\eta = 5.61953 \times 10^{-1}$, one generalize d Hopf bifurcation point $GH(1.11918 \times 10^1, 3.27432 \times 10^1)$ as $\mathcal{K} = 2.01991 \times 10^1$, $\eta = 3.59101 \times 10^{-1}$, See Fig. 3a. The transition of homoclinic cycle and heteroclinic cycle on the homoclinic bifurcation curve is illustrated by Fig. 3b. The whole phase plane is divided into five regions: $I - V$, its corresponding phase portraits are given in Fig. 4 as follows: (I) $\mathcal{K} = 19.9853$, $\eta = 0.39487$: a stable focus (11.3921,31.9489), a saddle (16.4041,27.5118); (II) $\mathcal{K} = 20.4433$, $\eta = 0.581991$: two stable nodes (0,0) and (20.4433,0), a saddle (2,0); (III) $\mathcal{K} = 20.199$, $\eta = 0.119345$: two coexistent limit cycles. We find that the outermost= is stable

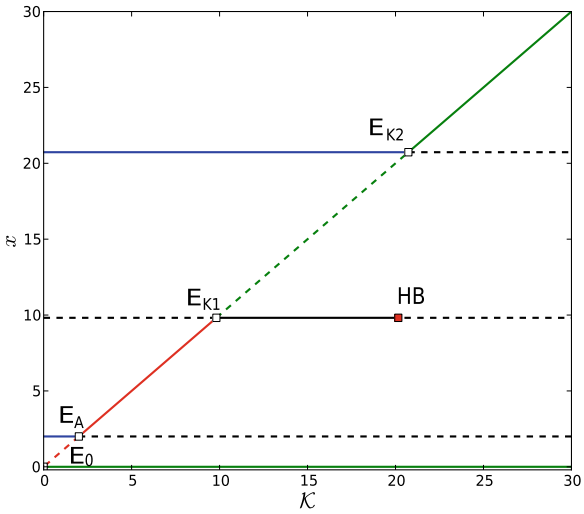

Fig. 2 Schematic bifurcation diagram for the carrying capacity $\mathcal{K}$, where $E_0, E_A, E_{\mathcal{K}1}, E_{\mathcal{K}2}, HB$ denote the boundary equilibria and the subcritical Hopf bifurcation point. The solid line and the dotted line denote the stability and instability of equilibria

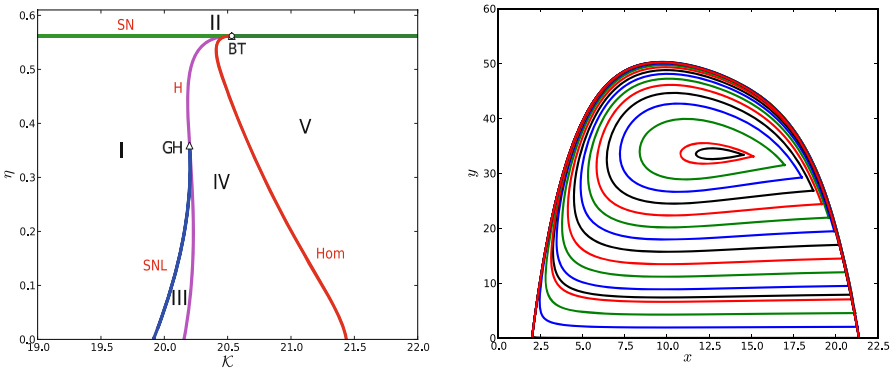

(a) (b)

Fig. 3 **a** Two-parameter bifurcation diagram of $\mathcal{K}$ versus η. Here SN, H, Hom, SNL denote Hopf bifurcation curve, saddle-node bifurcation curve, homoclinic bifurcation curve, and saddle-node bifurcation curve of limit cycle, respectively. **b** A family of homoclinic cycles are approaching a heteroclinic cycle as $\mathcal{K}$ and η varied

while the innermost is unstable which encloses a stable focus (10.1869,32.7504); (IV) $\mathcal{K} = 20.4191$, $\eta = 0.554912$: a homoclinic cycle which is homoclinic to a saddle point (14.0389,33.6241), enclosing a stable limit cycle and an unstable focus (13.0607,33.7165); (V) $\mathcal{K} = 21.0617$, $\eta = 0.416971$: an unstable focus (11.5282,36.0019) and a saddle (16.1621,36.1542). Biologically speaking, the collapse of the predator–prey system may occur once the intensity of anti-predator behavior overpasses the threshold $\eta = 5.61953 \times 10^{-1}$, whether the carrying capacity of prey is small or large.

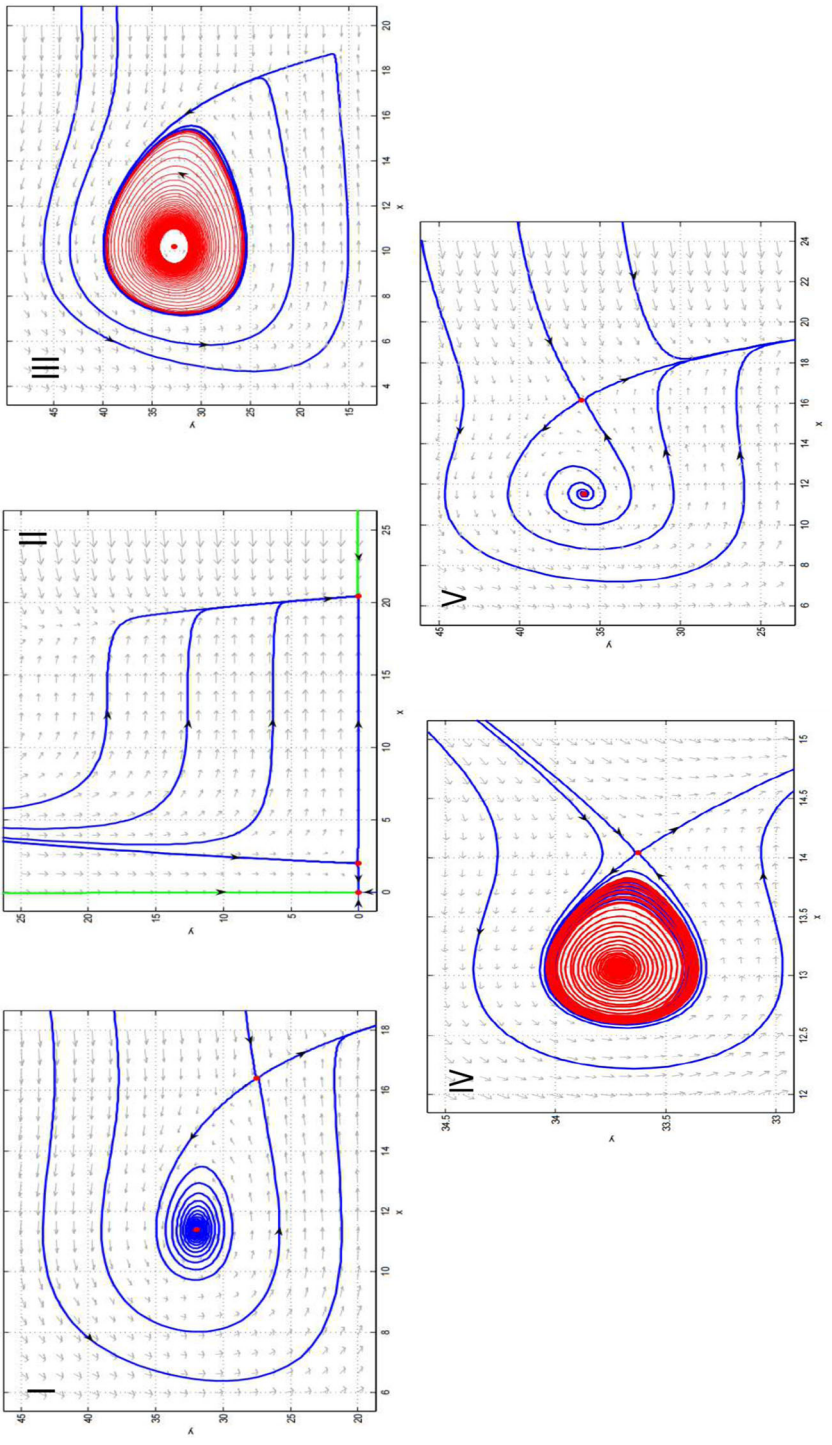

Fig. 4 Phase portraits in regions $I - VI$ of Fig. 3a

5.2 *d* and *b* as the Bifurcation Parameters

When the death rate of the predator (d) is used as the bifurcation parameter, we have two boundary equilibria $(2.0, 0)$ as $d = 2.48439$, $(2.0 \times 10^1, 0)$ as $d = 2.54167 \times 10^1$, one saddle-node bifurcation point $SN(1.42714 \times 10^1, 3.12627 \times 10^1)$ as $d = 3.20196 \times 10^1$, and one supercritical Hopf bifurcation point $HB(9.40803, 3.21331 \times 10^1)$ as $d = 2.29264 \times 10^1$. The limit cycle branch bifurcating from HB has one saddle-node bifurcation point $SN(1.36760 \times 10^1, 3.80390 \times 10^1)$ as $d = 2.47903 \times 10^1$, $period = 1.37125 \times 10^{-1}$.

When the death rate of the predator (d) and the intensity of group defense (b) are used as the bifurcation parameters, we have one Hopf bifurcation curve H with one generalized Hopf bifurcation point $GH(1.09319 \times 10^1, 3.29125 \times 10^1)$ as $d = 2.68479 \times 10^1, b = -1.07925 \times 10^{-1}$, one Bogdanov–Takens bifurcation point $BT(1.36527 \times 10^1, 3.06267 \times 10^2)$ as $d = 3.22885, b = 1.63083 \times 10^{-1}$, one saddle-node bifurcation curve SN, one homoclinic cycle bifurcation curve Hom, one saddle-node bifurcation curve of limit cycle SNL. See Fig. 5a. Note that the homoclinic cycle bifurcation curve exhibits the transition of homoclinic cycles as d and b varied, see Fig. 5b. The whole phase plane is divided into six regions: $I - VI$, its corresponding phase portraits are given in Fig. 6 as follows: (I) $d = 19.7269$, $b = -0.116389$: one unstable limit cycle which encloses a stable focus (7.7555,27.6516); (II) $d = 23.2225$, $b = -0.109456$: two coexistent limit cycles. The outermost one is stable, and the innermost one is unstable, which encloses a stable focus (9.4093,31.73); (III) $d = 22.5396$, $b = -0.123055$: one stable focus (10.1869,32.7504); (IV) $d = 20.0255$, $b = -0.0927508$: a homoclinic cycle enclosing an unstable focus (11.8376,47.3267), which is homoclinic to a saddle (17.1792,36.5751); (V) $d = 16.3239$, $b = -0.0721518$: no positive equilibrium; (VI) $d = 27.6419$, $b = -0.104496$: a stable focus (13.1043,36.2149) and a saddle (15.5371,33.863). From a biological viewpoint, the predator and the prey may undergo extinction finally by undergoing saddle-node bifurcation if the intensity of group defense is high and the natural mortality rate of the predator is small, or with a weak intensity of group defense and a large natural mortality rate of the predator.

5.3 *A* and *η* as the Bifurcation Parameters

When the strong Allee effect of the prey (A) and the intensity of anti-predator behavior (η) are used as the bifurcation parameters, we have a two-parameter bifurcation diagram including Hopf bifurcation curve H, saddle-node bifurcation curve of equilibrium SN, saddle-node bifurcation curve of limit cycle SNL, homoclinic cycle bifurcation Hom. There are one generalized Hopf bifurcation point $GH(1.10423 \times 10^1, 3.13170 \times 10^1)$ as $A = 2.20176, \eta = 3.29880 \times 10^{-1}$, and one Bogdanov–Takens bifurcation point $BT(1.35362 \times 10^1, 2.78704 \times 10^1)$ as $A = 3.37915, \eta = 5.61953 \times 10^{-1}$. The homoclinic cycles on the homoclinic branch are approaching a heteroclinic cycle. The homoclinic cycles are homoclinic to the right equilibrium and finally become one heteroclinic cycle connecting two boundary equilibria. See Fig. 7a, b. The whole phase plane is divided into five regions: $I - V$,

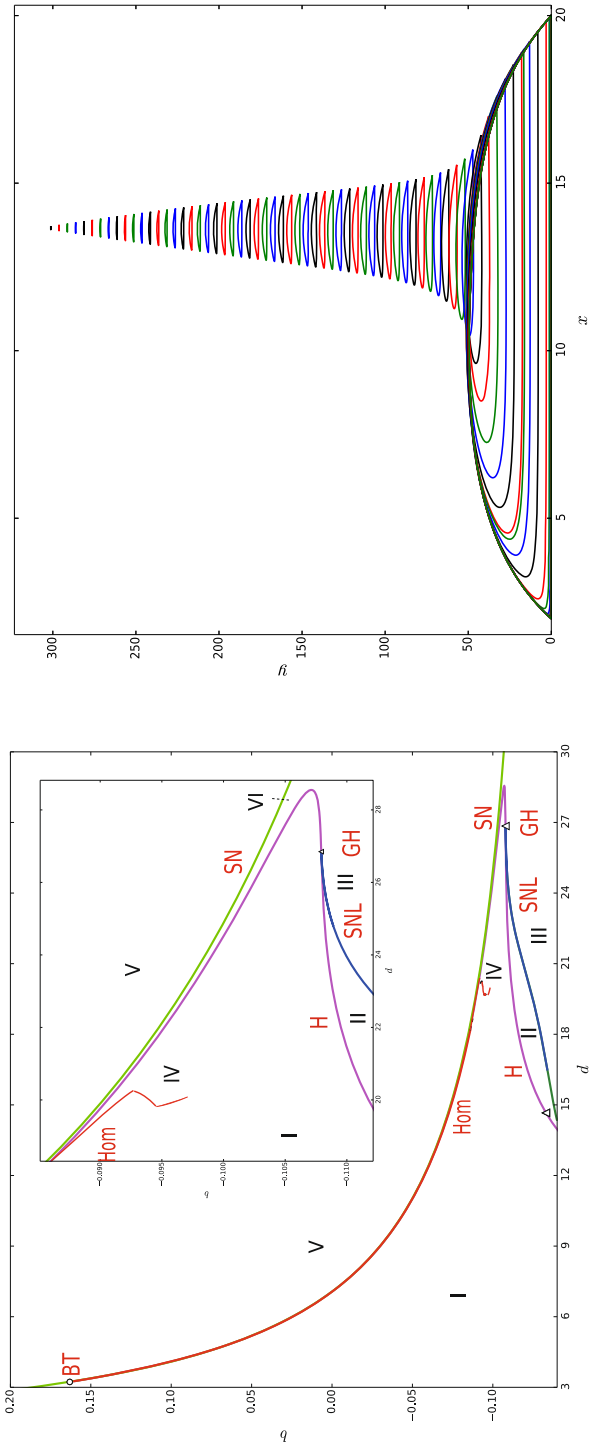

Fig. 5 **a** Two-parameter bifurcation diagram of d versus b. Here SN, H, Hom, SNL denote saddle-node bifurcation curve, Hopf bifurcation curve, homoclinic bifurcation curve, and saddle-node bifurcation curve of limit cycle, respectively. **b** The transition of homoclinic cycles as d and b varied

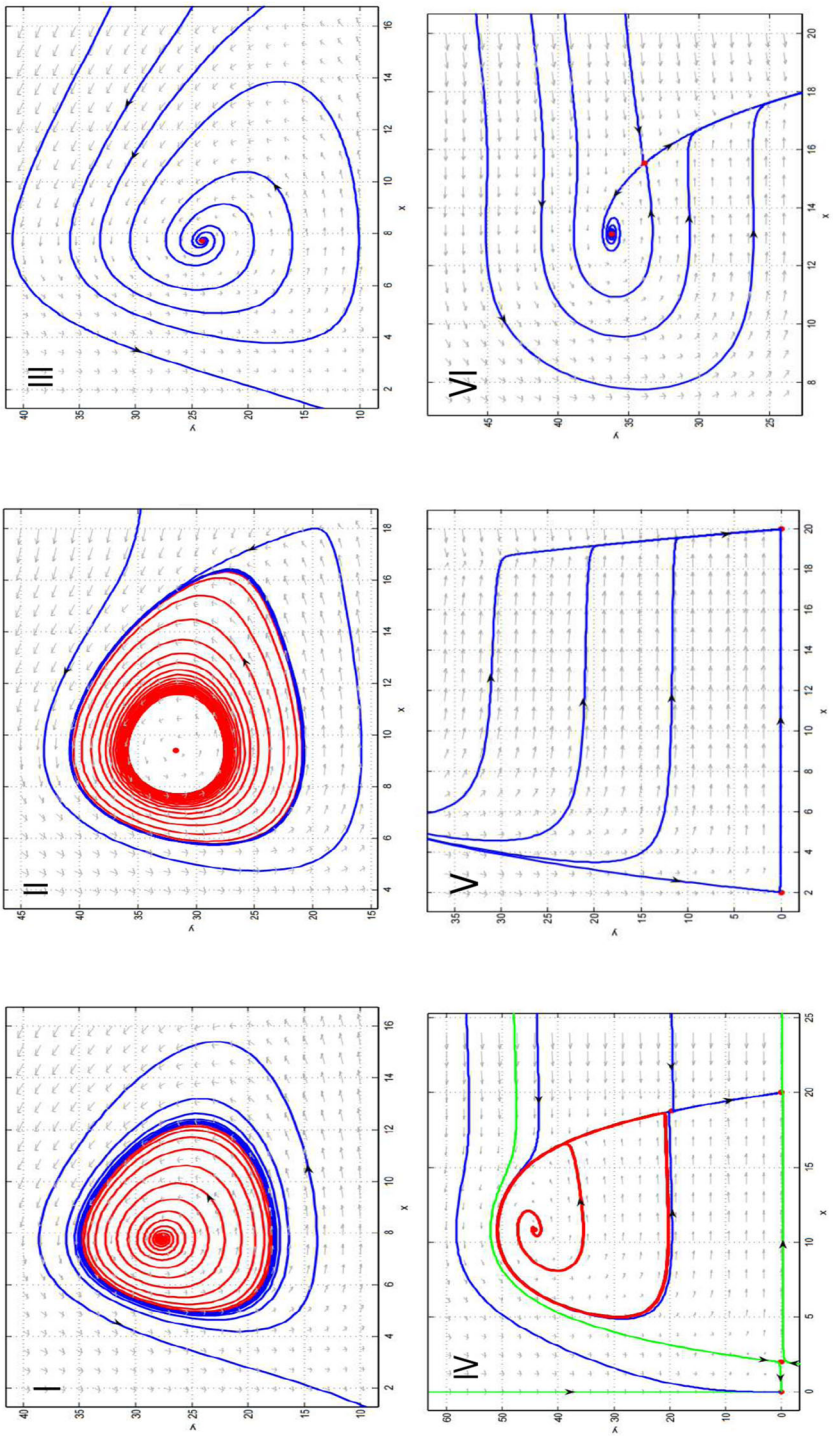

Fig. 6 Phase portraits in regions I–V of Fig. 5a

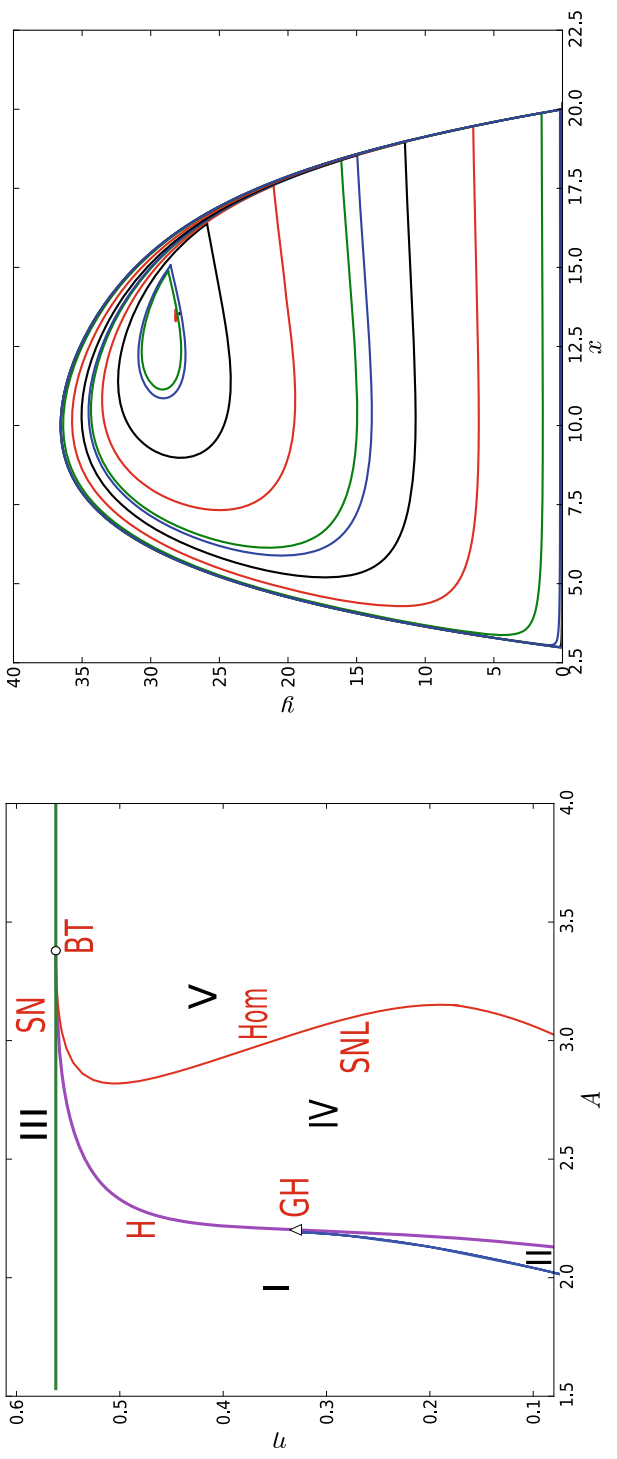

Fig. 7 **a** Two-parameter bifurcation diagram of A versus η. **b** The transition of homoclinic cycle and heteroclinic cycle as A and η varied. Here SN, H, Hom, SNL denote saddle-node bifurcation curve, Hopf bifurcation curve, homoclinic bifurcation curve and saddle-node bifurcation curve of limit cycle, respectively

its corresponding phase portraits are given in Fig. 8 as follows: (I) $A = 1.85697$, $\eta = 0.314403$: a stable focus (10.9674,32.5487) and a saddle (17.2468,24.6032); (II) $A = 2.10324$, $\eta = 0.112899$: two infinitesimal limit cycles. The outermost one is stable, and the innermost one is unstable and encloses a stable focus (10.1647,31.6951); (III) $A = 2.4956$, $\eta = 0.574837$: no positive equilibrium; (IV) $A = 2.88379$, $\eta = 0.420858$: a saddle homoclinic cycle is homoclinic to a saddle (14.1939,28.3504), and encloses an unstable focus (12.9243,28.4606); (V) $A = 3.1551$, $\eta = 0.550125$: an unstable focus (12.9243,28.4606) and a saddle (14.1939,28.3504).

The biological implication is similar to that with the effect of the carrying capacity. The collapse of the predator–prey system may occur once the intensity of anti-predator behavior overpasses the same threshold of $\eta = 5.61953 \times 10^{-1}$, whether the strong Allee effect of prey is small or large. However, we find that the existence of a heteroclinic orbit connecting two boundary equilibria $E_A(A, 0)$ and $E_K(K, 0)$, which indicates that the predator population may go through extinction even with the small intensity of anti-predator behavior due to the involvement of a strong Allee effect.

5.4 The Role of Weak Allee Effect

We consider the role of the weak Allee effect by using a new set of parameter values in Arsie et al. [21] as follows

$$\begin{aligned} &\mathcal{K} = 10.5, A = -0.5, a = 0.01809954751, b = -0.1809954751, \\ &d = 8.99, \eta = 0.005. \end{aligned} \tag{68}$$

When the intensity of group defense (b) is taken as the bifurcation parameter, we have one supercritical Hopf bifurcation point $HB(6.40842, 2.00778 \times 10^1)$ as $b = -1.61195 \times 10^{-1}$, and a saddle-node bifurcation point $SN(7.42047, 2.00502 \times 10^1)$ as $b = -1.58292 \times 10^{-1}$.

When the death rate of the predator (d) and the intensity of group defense (b) are the primary bifurcation parameters, we obtain the two-parameter bifurcation diagram including saddle-node bifurcation curve SN, Hopf bifurcation curve H, saddle-node bifurcation curve of limit cycle SNL, and one homoclinic cycle bifurcation curve Hom. There are one Bogdanov–Takens bifurcation point $BT(6.88640, 1.42079 \times 10^2)$ as $b = 5.03122 \times 10^{-1}$, $d = 1.25927$, and the heteroclinic cycle connecting $(0, 0)$ and $(10.5, 0)$. In particular, the saddle-node bifurcation curve of limit cycle SNL has one codimension-2 cusp CPL of limit cycle, which indicates that there are coexistent three limit cycles, see Fig. 9a. The transition between the homoclinic cycle and the heteroclinic cycle is illustrated by Fig. 9b. The whole phase plane is divided into five regions: $I - V$, its corresponding phase portraits are given in Fig. 10 as follows: (I) there are two kinds of situation in this region: (a) $d = 4.32258$, $b = -0.213085$: two coexistent limit cycles. The outermost one is stable, and the innermost one is unstable, which encloses a stable focus (2.51055,13.9293); (b) $d = 3.78893$, $b = -0.220932$: three coexistent limit cycles. The outermost one and the innermost one are stable, the middle one is unstable, and the innermost one encloses an unstable focus (2.2561,13.4891); (II) $d = 6.42346$, $b = -0.198362$: a stable focus (3.43,14.7972); (III) $d = 5.1964$,

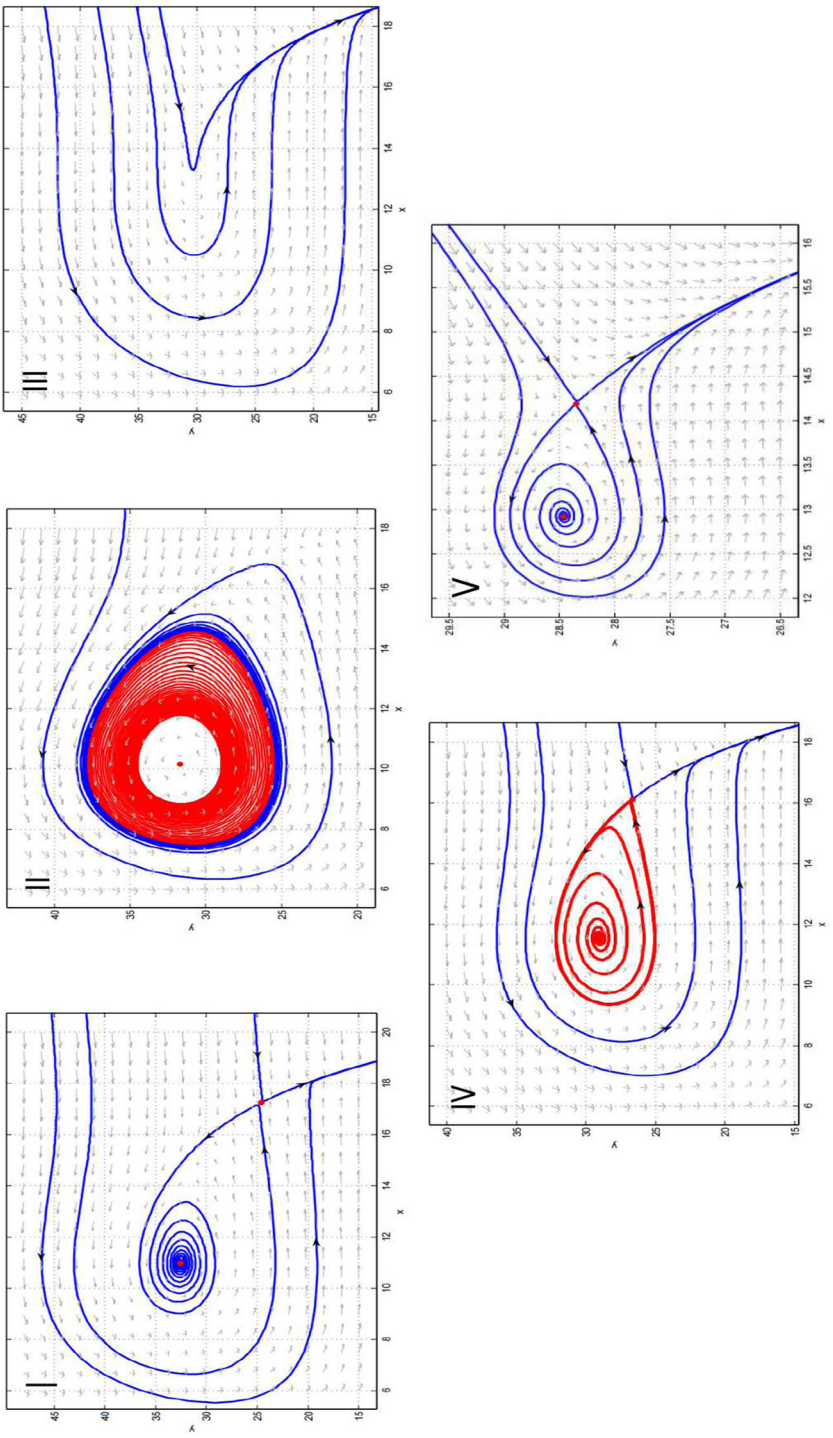

Fig. 8 Phase portraits in regions I–V of Fig. 7b

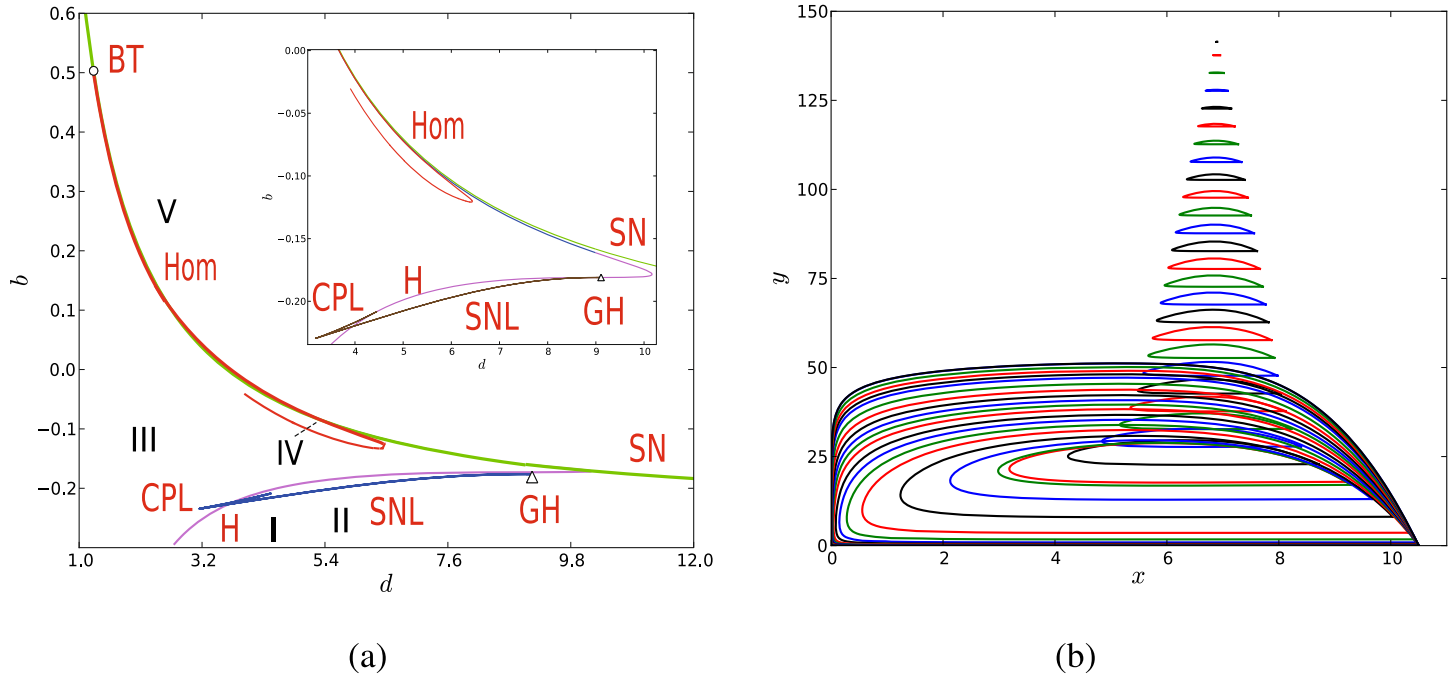

Fig. 9 **a** Two-parameter bifurcation diagram of d versus b for the weak Allee effect. Here SN, H, Hom, SNL denote saddle-node bifurcation curve, Hopf bifurcation curve, homoclinic bifurcation curve and saddle-node bifurcation curve of limit cycle, respectively. **b** The transition of homoclinic cycles as b and d vary

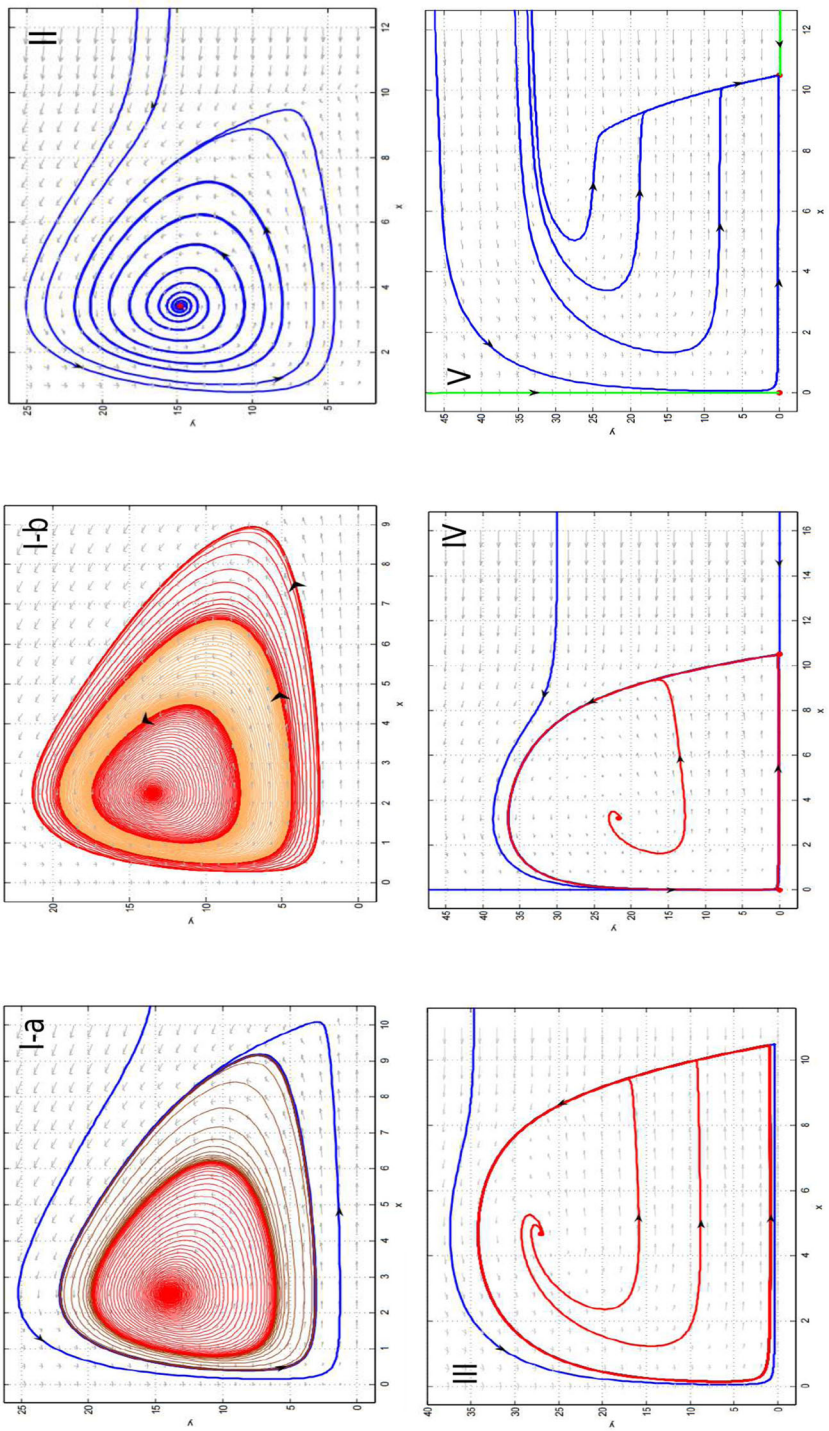

Fig. 10 Phase portraits in regions I–V of Fig. 9a

$b = -0.106871$: an unstable focus (4.67751,27.0142) which will approach a homoclinic cycle; (IV) $d = 3.99, b = -0.12$: an unstable focus (3.21,21.672) and a saddle heteroclinic cycle is heteroclinic to two saddles (0,0) and (10.5,0); There is an attracting separatrix representing a critical curve which has to trespass for the predator. (V) $d = 6.53501, b = -0.1095$: no positive equilibrium.

Note that, based on the normal form of codimension-2 cusp of the limit cycle in (66) and with the help of Matcont [55], we obtain the coefficient value $c = -9.671688 < 0$ as $d = 3.181119, b = -2.295880 \times 10^{-1}$, and $period = 9.968795 \times 10^{-1}$ in Fig. 9a. It indicates that there are coexistent three limit cycles bifurcating from one Hopf bifurcation point. Moreover, there exists a parameter region for two limit cycles and a parameter region for three limit cycles in the acute angle region of the cusp point CPL. However, it is not easy to locate the boundary between them.

Remark 1 Based on the above analysis, we find that the strong Allee effect may cause the coexistence of two limit cycles while the weak Allee effect may cause the coexistence of three limit cycles.

Remark 2 The whole bifurcation diagram will move to the lower right corner as the intensity of anti-predator behavior η increases while keeping the bifurcation structure unchanged. For example, if we choose $\eta = 0.3$, then there are one Bogdanov–Takens bifurcation point $BT(1.32797 \times 10^1, 5.08500 \times 10^1)$ as $d = 1.58124 \times 10^1, b = -8.99253 \times 10^{-2}$, and one generalized Hopf bifurcation point $GH(1.09266 \times 10^1, 3.29115 \times 10^1)$ as $d = 2.36122 \times 10^1, b = -1.07926 \times 10^{-1}$. However, if $\eta = 0.005$, then there are one Bogdanov–Takens bifurcation point $BT(1.36527 \times 10^1, 3.06267 \times 10^2)$ when $d = 3.22885, b = 1.63083 \times 10^{-1}$, and one generalized Hopf bifurcation point $GH(1.09319 \times 10^1, 3.29125 \times 10^1)$ as $d = 2.68479 \times 10^1, b = -1.07925 \times 10^{-1}$.

Remark 3 The coexistence of two limit cycles in the predator–prey system is found in the existing literature. However, the codimension-2 cusp of the limit cycle indicating the coexistence of three limit cycles is rarely studied in the predator–prey system with the Allee effect. The mechanism of the limit cycle is different from that in Aguirre et al. [36].

Remark 4 Note that Aguirre et al. [36] found three limit cycles in a Leslie-Gower predator–prey with Allee effect, the first two limit cycles originating from Hopf bifurcation and the third one arising from a homoclinic bifurcation. They are surrounded by different equilibria. Actually, the first two small limit cycles bifurcate from one Hopf bifurcation point and disappear at another Hopf bifurcation point, while the third limit cycle bifurcates from one Hopf bifurcation point and a family of periodic orbits approaches a homoclinic cycle or arises from a perturbed homoclinic cycle. The generating mechanism of the third limit cycle is the same as the scenario of [41, 56].

6 Biological Interpretations

In this section, we provide biological interpretations on the basis of phase portraits of two-parameter bifurcation diagrams under the assumption that the initial conditions

are taken biologically meaningful. We consider the regimes where the trajectories are stable for the initial conditions chosen outside the stable or unstable manifolds of equilibrium, and not on an unstable limit cycle, which indicates that the final regime will be the same if small changes perturb the initial conditions. There are three kinds of stable regimes as described below.

(1) The regime with the extinction of the predator (REP), where there is an open set of initial conditions in which the predator goes extinct, and the prey is at a stable steady state. The phase portraits for the open region II in Fig. 3a, the open region V in Fig. 5a, the open region III in Fig. 7b, and the open region V in Fig. 9a correspond to the stable regime REP with both prey and predator converging to the stable boundary equilibria $(A, 0)$ or $(K, 0)$, i.e., the predator will eventually go extinct.
(2) The regime of multiple equilibria (RME), where the prey and the predator coexist, tending to their stable equilibria. The phase portraits for regime III in Fig. 3a, regime II in Fig. 5a and regime II in Fig. 7b, regime I(i) in Fig. 9a correspond to the stable regime RME in a small region bounded by the interior of the limit cycle.
(3) The regime of oscillation (RO), where there is an open set of the initial conditions for both the prey and the predator to tend to a stable oscillatory regime, i.e., a stable limit cycle. See regime IV in Fig. 3a, regime II in Fig. 5a, regime I in Fig. 7b, regime I(ii) in Fig. 9a, where we find this kind of stable regime RO.

Based on the above observations, we can make the following conclusions.

(a) The increasing intensity of anti-predator behavior can move the whole bifurcation diagram to the lower right corner while keeping the dynamics unchanged. However, it may cause the predator to go extinct even with the large carrying capacity of the prey.
(b) Strong Allee effect and weak Allee effect have a similar effect on the predator–prey system as the intensity of group defense and the natural death rate of the predator vary. The strong Allee effect could cause the predator to undergo extinction even with the smaller intensity of the anti-predator.
(c) The increasing intensity of group defense could cause the predator to become extinct even with a smaller death rate of the predator due to the emergence of a heteroclinic cycle connecting two boundary equilibria.

Conclusion and Discussion

In this paper, we have studied the global dynamics of a predator–prey model with the Allee effect and the anti-predator behavior by using the dynamical systems approach. We have shown the existence of saddle-node bifurcation, Hopf bifurcation of codimension 3, homoclinic bifurcation, heteroclinic bifurcation, Bogdanov–Takens bifurcation of codimension 3, saddle-node bifurcation of limit cycle, and codimension-2 cusp of limit cycle. The results found in this paper reveal that the transition from the coexistence of prey and predator to the extinction of the predator in a predator–prey model can generate more complex dynamics, including the coexistence of three limit cycles for the weak Allee effect and two coexistent limit cycles for the strong Allee effect.

It is worth noting that a strong Allee effect may also cause multiple limit cycles to generate under appropriate parameter values.

Our study also showed that the codimension-2 cusp of the infinitesimal limit cycle leads to more complex dynamics, including homoclinic cycle bifurcation and heteroclinic cycle bifurcation, and saddle-node bifurcation of the limit cycle. It indicates that the mechanism of the limit cycle is different from that in Aguirre et al. [36], where the first two limit cycles are infinitesimal and the third one arises from a homoclinic cycle. As far as we know, it is the first time to find the codimension-2 cusp of limit cycle in a predator–prey system with the Allee effect. Based on the observations of the bifurcation diagrams and their corresponding phase portraits, an important conclusion is obtained: if the intensity of the anti-predator is fixed, then the strong Allee effect and the weak Allee effect have the similar effect on the predator–prey system as the intensity of group defense and the natural death rate of the predator vary. The anti-predator behavior may cause the predator to become extinct even with the small carrying capacity of the prey. The strong Allee effect could cause the predator to go extinct even with the smaller intensity of the anti-predator. The transition from the homoclinic cycle to the heteroclinic cycle indicates the collapse of the predator–prey system and the extinction of the predator.

Lastly, the degenerate homoclinic bifurcation point in the saddle-node bifurcation curve of the limit cycle is not found since it actually connects two codimension-2 degenerate Hopf bifurcation points. Although we have located the possible coexistence region of two limit cycles and the coexistence region of three limit cycles, it is challenging to identify the boundary between them, which is left for future research.

Acknowledgements The authors are very grateful to the anonymous reviewers for their valuable and insightful suggestions. YX was partially supported by the National Natural Science Foundation of China (No. 11671114). LR is supported by the National Science Foundation Grant DMS-1950254.

Author Contributions TW and YX wrote the main manuscript text, MH and LR prepared all figures. All authors reviewed the manuscript.

Declarations

Conflict of interest The authors declare that they have no conflict of interest.

Appendix A

$$\gamma_1 = \frac{\left(ax_*^2 + bx_* + 1\right)\left(a^2x_*^3 - 3ax_* - b\right)}{x_*\left(3a^2x_*^2 + 3abx_* - a + b^2\right)},$$

$$\gamma_2 = \frac{1}{x_*\left(ax_*^2 + bx_* + 1\right)} - \frac{ax_*}{ax_*^2 + bx_* + 1},$$

$$\gamma_3 = \frac{-2a^3x_*^5 + 10a^2x_*^3 + 5abx_*^2 - 4ax_* + b^2x_* - b}{x_*^2\left(3a^2x_*^2 + 3abx_* - a + b^2\right)},$$

$$\gamma_4 = \frac{-a^2x_*^3 + 3ax_* + b}{x_*\left(ax_*^2 + bx_* + 1\right)^2} + \frac{3\left(4a^3x_*^3 + 6a^2bx_*^2 - 4a^2x_* + 4ab^2x_* - 2ab + b^3\right)}{3a^2x_*^2 + 3abx_* - a + b^2},$$

$$\gamma_5 = \frac{a^2x_*^4 - 4ax_*^2 - 2bx_* - 1}{x_*^2\left(ax_*^2 + bx_* + 1\right)^2},$$

$$\gamma_6 = \frac{3a^4x_*^6 - 23a^3x_*^4 - 16a^2bx_*^3 + 21a^2x_*^2 - 6ab^2x_*^2 + 12abx_* - a - b^3x_* + 2b^2}{x_*^2\left(ax_*^2 + bx_* + 1\right)\left(3a^2x_*^2 + 3abx_* - a + b^2\right)},$$

$$\gamma_7 = \frac{a^2 - 2a(b-3)b + (b-3)b^3}{x_*\left(a - b^2\right)} + \frac{b\left(a\left(bx_* - 2\right) + b^2\right)}{\left(x_*\left(ax_* + b\right) + 1\right)^2} + \frac{\left(b^2 - 4a\right)(2ax_* + b)}{\left(x_*\left(ax_* + b\right) + 1\right)^3}$$
$$- \frac{a^2\left(-x_*\right) + a\left(b\left(bx_* - 1\right) + 12\right) + (b-3)b^2}{x_*\left(ax_* + b\right) + 1}$$
$$+ \frac{a\left(4a - b^2\right)\left(3abx_* + a + 2b^2\right)}{\left(a - b^2\right)\left(a\left(3x_*\left(ax_* + b\right) - 1\right) + b^2\right)},$$

$$\gamma_8 = \frac{-a^3x_*^6 + 9a^2x_*^4 + 9abx_*^3 + 3ax_*^2 + 3b^2x_*^2 + 3bx_* + 1}{x_*^3\left(ax_*^2 + bx_* + 1\right)^3}.$$

Appendix B

$$\delta_1 = \frac{\left(ax_*^2 - 1\right)(A - x_*)(x_* - \mathcal{K})}{ax_*^2 + bx_* + 1} - A\mathcal{K} + 2Ax_* + 2\mathcal{K}x_* - 3x_*^2,$$

$$\delta_2 = -\frac{x_*}{ax_*^2 + bx_* + 1}, \delta_3 = -\frac{(A - x_*)(x_* - \mathcal{K})\left(a^2x_*^3 - 3ax_* - b\right)}{\left(ax_*^2 + bx_* + 1\right)^2}$$
$$+ A + \mathcal{K} - 3x_*,$$

$$\delta_4 = \frac{ax_*^2 - 1}{\left(ax_*^2 + bx_* + 1\right)^2},$$

$$\delta_5 = \frac{\left(-a^3x_*^4 + 6a^2x_*^2 + 4abx_* - a + b^2\right)\left(A\mathcal{K} - Ax_* - \mathcal{K}x_* + x_*^2\right)}{\left(ax_*^2 + bx_* + 1\right)^3} - 1,$$

$$\delta_6 = \frac{-a^2x_*^3 + 3ax_* + b}{\left(ax_*^2 + bx_* + 1\right)^3}, \delta_7 = \frac{(x_* - A)(\mathcal{K} - x_*)\left(a^2x_*^3 - 3ax_* - b\right)}{\left(ax_*^2 + bx_* + 1\right)^2},$$

$$\delta_8 = \frac{a^2x_*^3 - 3ax_* - b}{\left(ax_*^2 + bx_* + 1\right)^3},$$

$$\delta_9 = \frac{(x_* - A)(\mathcal{K} - x_*)\left(-a^3x_*^4 + 6a^2x_*^2 + 4abx_* - a + b^2\right)}{\left(ax_*^2 + bx_* + 1\right)^3}.$$

Appendix C

$$\epsilon_1 = \frac{(x_* - A)(\mathcal{K} - x_*)\left(a^2x_*^3 - 3ax_* - b\right)}{\left(ax_*^2 + bx_* + 1\right)^2},$$

$$\epsilon_2 = \frac{a^2x_*^2(-A\mathcal{K} + 2Ax_* + 2\mathcal{K}x_*) - 3a^2x_*^4 + x_*\left(-4a(A+\mathcal{K}) + 7ax_* + 2b\right) + A(a\mathcal{K} - b) - b\mathcal{K}}{\left(ax_*^2 + bx_* + 1\right)^2},$$

$$\epsilon_3 = \frac{a^2x_*^3 - 3ax_* - b}{\left(ax_*^2 + bx_* + 1\right)^3},$$

$$\begin{aligned}\epsilon_4 = \frac{1}{\left(ax_*^2 + bx_* + 1\right)^2}(&-24a^3x_*^8 + 30a^3Ax_*^7 - 54a^2bx_*^7 + 30a^3\mathcal{K}x_*^7 - 40a^2x_*^6 - 9a^3A^2x_*^6\\
&- 39ab^2x_*^6 - 9a^3\mathcal{K}^2x_*^6 + 64a^2Abx_*^6 - 34a^3A\mathcal{K}x_*^6 + 64a^2b\mathcal{K}x_*^6 - 9b^3x_*^5 - a^2x_*^5 + 43aAb^2x_*^5\\
&+ 9a^3A\mathcal{K}^2x_*^5 - 18a^2b\mathcal{K}^2x_*^5 + 45a^2Ax_*^5 - 18a^2A^2bx_*^5 - 55abx_*^5 + 45a^2\mathcal{K}x_*^5 + 9a^3A^2\mathcal{K}x_*^5\\
&+ 43ab^2\mathcal{K}x_*^5 - 67a^2Ab\mathcal{K}x_*^5 + 9Ab^3x_*^4 - 12a^2A^2x_*^4 - 11aA^2b^2x_*^4 - 18b^2x_*^4 - 12a^2\mathcal{K}^2x_*^4\\
&- 2a^3A^2\mathcal{K}^2x_*^4 - 11ab^2\mathcal{K}^2x_*^4 + 16a^2Ab\mathcal{K}^2x_*^4 - 18ax_*^4 + a^2Ax_*^4 + 56aAbx_*^4 + 9b^3\mathcal{K}x_*^4\\
&- 40aAb^2\mathcal{K}x_*^4 - 44a^2A\mathcal{K}x_*^4 + 16a^2A^2b\mathcal{K}x_*^4 + 56ab\mathcal{K}x_*^4 - 2A^2b^3x_*^3 + 16Ab^2x_*^3 - 2b^3\mathcal{K}^2x_*^3\\
&+ 8aAb^2\mathcal{K}^2x_*^3 + 10a^2A\mathcal{K}^2x_*^3 - 3a^2A^2b\mathcal{K}^2x_*^3 - 13ab\mathcal{K}^2x_*^3 + 3ax_*^3 + 16aAx_*^3 - 13aA^2bx_*^3\\
&- 11bx_*^3 - 7Ab^3\mathcal{K}x_*^3 + 10a^2A^2\mathcal{K}x_*^3 + 8aA^2b^2\mathcal{K}x_*^3 + 16b^2\mathcal{K}x_*^3 + 16a\mathcal{K}x_*^3 - a^2A\mathcal{K}x_*^3 + a^2\mathcal{K}x_*^4\\
&- 46aAb\mathcal{K}x_*^3 - 3aA^2x_*^2 - 3A^2b^2x_*^2 + Ab^3\mathcal{K}^2x_*^2 - 2a^2A^2\mathcal{K}^2x_*^2 - aA^2b^2\mathcal{K}^2x_*^2 - 3b^2\mathcal{K}^2x_*^2\\
&- 3a\mathcal{K}^2x_*^2 + 8aAb\mathcal{K}^2x_*^2 - 3aAx_*^2 + 8Abx_*^2 + bx_*^2 + A^2b^3\mathcal{K}x_*^2 - 10Ab^2\mathcal{K}x_*^2 - 3a\mathcal{K}x_*^2 + Ax_*\\
&- 10aA\mathcal{K}x_*^2 + 8aA^2b\mathcal{K}x_*^2 + 8b\mathcal{K}x_*^2 - 2x_*^2 + Ab^2\mathcal{K}^2x_* + aA\mathcal{K}^2x_* - aA^2b\mathcal{K}^2x_* - b\mathcal{K}^2x_*\\
&- A^2bx_* - Abx_* + aA^2\mathcal{K}x_* + A^2b^2\mathcal{K}x_* + 3aA\mathcal{K}x_* - 3Ab\mathcal{K}x_* - b\mathcal{K}x_* + \mathcal{K}x_* + Ab\mathcal{K}),\end{aligned}$$

$$\epsilon_5 = \frac{(x_*\left(-3x_*(a(A+\mathcal{K}) - b) + 2aA\mathcal{K} + 4ax_*^2 - 2Ab - 2b\mathcal{K} + 2\right) + A(b\mathcal{K} - 1) - \mathcal{K})(ax_*^2 - 1)}{\left(ax_*^2 + bx_* + 1\right)^2},$$

$$\begin{aligned}\epsilon_6 = \frac{1}{\left(ax_*^2 + bx_* + 1\right)^2}(&8a^3x_*^7 - 14a^3Ax_*^6 - 2a^2bx_*^6 - 14a^3\mathcal{K}x_*^6 - 32a^2x_*^5 + 6a^3A^2x_*^5 - A^2b\\
&+ 6a^3\mathcal{K}^2x_*^5 - 4a^2Abx_*^5 + 20a^3A\mathcal{K}x_*^5 - 4a^2b\mathcal{K}x_*^5 - 3b^3x_*^4 - 3a^2x_*^4 + 7aAb^2x_*^4 - 7a^3A\mathcal{K}^2x_*^4\\
&+ 4a^2b\mathcal{K}^2x_*^4 + 37a^2Ax_*^4 + 4a^2A^2bx_*^4 - 47abx_*^4 + 37a^2\mathcal{K}x_*^4 - 7a^3A^2\mathcal{K}x_*^4 + 7ab^2\mathcal{K}x_*^4 - b\mathcal{K}^2\\
&+ 9a^2Ab\mathcal{K}x_*^4 + 2Ab^3x_*^3 - 10a^2A^2x_*^3 - 14b^2x_*^3 - 10a^2\mathcal{K}^2x_*^3 + 2a^3A^2\mathcal{K}^2x_*^3 - 4a^2Ab\mathcal{K}^2x_*^3\\
&- 22ax_*^3 + 2a^2Ax_*^3 + 48aAbx_*^3 + 2b^3\mathcal{K}x_*^3 + 2a^2\mathcal{K}x_*^3 - 4aAb^2\mathcal{K}x_*^3 - 40a^2A\mathcal{K}x_*^3 - aA^2b\mathcal{K}^2\\
&+ 48ab\mathcal{K}x_*^3 + 12Ab^2x_*^2 + 10a^2A\mathcal{K}^2x_*^2 + a^2A^2b\mathcal{K}^2x_*^2 - 11ab\mathcal{K}^2x_*^2 + 7ax_*^2 + 20aAx_*^2 - Ab\\
&- 11aA^2bx_*^2 - 11bx_*^2 - Ab^3\mathcal{K}x_*^2 + 10a^2A^2\mathcal{K}x_*^2 + 12b^2\mathcal{K}x_*^2 + 20a\mathcal{K}x_*^2 - a^2A\mathcal{K}x_*^2 + aA^2\mathcal{K}\\
&- 4aA^2x_* - 2A^2b^2x_* - 2a^2A^2\mathcal{K}^2x_* - 2b^2\mathcal{K}^2x_* - 4a\mathcal{K}^2x_* + 8aAb\mathcal{K}^2x_* - 4aAx_* + 8Abx_*\\
&+ 2bx_* - 8Ab^2\mathcal{K}x_* - 4a\mathcal{K}x_* - 12aA\mathcal{K}x_* + 8aA^2b\mathcal{K}x_* + 8b\mathcal{K}x_* - 2x_* + Ab^2\mathcal{K}^2 + aA\mathcal{K}^2\\
&- 42aAb\mathcal{K}x_*^2 + A^2b^2\mathcal{K} + aA\mathcal{K} - 3Ab\mathcal{K} - b\mathcal{K} + \mathcal{K}) - 10ab^2x_*^5 + A - 4a^2A^2b\mathcal{K}x_*^3,\end{aligned}$$

$$\epsilon_7 = \frac{Ab^2\mathcal{K} - Ab - b\mathcal{K} - b}{(ax_*^2 + bx_* + 1)^3} + \frac{x_*\left(5aAb\mathcal{K} - 3aA - 3a\mathcal{K} - 3a - 2Ab^2 - 2b^2\mathcal{K} + 2b\right)}{(ax_*^2 + bx_* + 1)^3}$$

$$
\begin{aligned}
&+\frac{x_*^2\left(6a^2A\mathcal{K}-9aAb-9ab\mathcal{K}+6a+3b^2\right)}{(ax_*^2+bx_*+1)^3}\\
&+\frac{x_*^3\left(-a^2Ab\mathcal{K}-8a^2A-8a^2\mathcal{K}+a^2+13ab\right)}{(ax_*^2+bx_*+1)^3}+\frac{x_*^4\left(-2a^3A\mathcal{K}+2a^2Ab+2a^2b\mathcal{K}+10a^2\right)}{(ax_*^2+bx_*+1)^3}\\
&+\frac{x_*^5\left(3a^3A+3a^3\mathcal{K}-3a^2b\right)-4a^3x_*^6}{(ax_*^2+bx_*+1)^3},\ (x_*)\\
&=\frac{x_*^2(2aA\mathcal{K}-2Ab-2b\mathcal{K}+2)+x_*(A(b\mathcal{K}-1)-\mathcal{K})}{ax_*^2+bx_*+1}+\frac{4ax_*^4-3x_*^3(a(A+\mathcal{K})-b)}{ax_*^2+bx_*+1}.
\end{aligned}
$$

References

1. Lotka, A.J.: The Elements of Physical Biology. Williams & Wilkins (1925)
2. Volterra, V.: Fluctuations in the abundance of species considered mathematically. Nature **119**(2983), 12–13 (1927)
3. Andrews, J.F.: A mathematical model for the continuous culture of microorganisms utilizing inhibitory substrates. Biotechnol. Bioeng. **10**(6), 707–723 (1968)
4. Zhu, H., Campbell, S.A., Wolkowicz, G.S.K.: Bifurcation analysis of a predator-prey system with nonmonotonic functional response. SIAM J. Appl. Math. **63**(2), 636–682 (2002)
5. Freedman, B.: Deterministic mathematical models in population ecology. Biometrics **22**(7), 219–236 (1980)
6. Gause, G.F.: Experimental analysis of Vito Volterra's mathematical theory of the struggle for existence. Science **79**(2036), 16–17 (1934)
7. Foster, W.A., Treherne, J.E.: Evidence for the dilution effect in the selfish herd from fish predation on a marine insect. Nature **293**(5832), 466–467 (1981)
8. Huang, J., Xiao, D.: Analyses of bifurcations and stability in a predator-prey system with Holling type-IV functional response. Acta Math. Appl. Sin. **20**(1), 167–178 (2004)
9. Myers, R.A., Worm, B.: Rapid worldwide depletion of large predatory fish communities. Nature **423**, 280–283 (2003)
10. Freedman, H.I., Wolkowicz, G.S.K.: Predator–prey systems with group defense: the paradox of enrochment revisted. Bull. Math. Biol. **8**, 493–508 (1996)
11. Xiao, D., Ruan, S.: Global analysis in a predator-prey system with nonmonotonic functional response. SIAM J. Appl. Math. **61**, 1445–1472 (2001)
12. Rothe, F., Shafer, D.S.: Multiple bifurcation in a predator-prey system with nonmonotonic predator response. Proc. R. Soc. Edinb. **120**, 313–347 (1992)
13. Naik, P.A., Eskandari, Z., Yavuz, M., Zu, J.: Complex dynamics of a discrete-time Bazykin–Berezovskaya prey-predator model with a strong Allee effect. J. Comput. Appl. Math. **413**, 114401 (2022)
14. Eskandari, Z., Avazzadeh, Z., Ghaziani, R.K.: Theoretical and numerical bifurcation analysis of a predator–prey system with ratio-dependence. Math. Sci. **3**, 1–2 (2023)
15. Li, B., Eskandari, Z., Avazzadeh, Z.: Strong resonance bifurcations for a discrete-time prey–predator model. J. Comput. Appl. Math. (2023). https://doi.org/10.1007/s12190-023-01842-2
16. Eskandari, Z., Avazzadeh, Z., Ghaziani, R.K., Li, B.: Dynamics and bifurcations of a discrete-time Lotka–Volterra model using nonstandard finite difference discretization method. Math. Methods Appl. Sci. (2022). https://doi.org/10.1002/mma.8859
17. Du, Y., Niu, B., Guo, Y., Wei, J.: Double Hopf bifurcation in delayed reaction–diffusion systems. J. Dyn. Differ. Equ. **32**, 313–358 (2020)
18. Duan, D., Niu, B., Wei, J.: Hopf–Hopf bifurcation and chaotic attractors in a delayed diffusive predator–prey model with fear effect. Chaos Solitons Fractals **123**, 206–216 (2019)
19. Allee, W.C.: Animal Aggregations: A Study in General Sociology. The University of Chicago Press (1931)

20. Allee, W.C.: An ecological audit. Ecology **20**(3), 418–421 (1939)
21. Arsie, A., Kottegoda, C., Shan, C.: A predator–prey system with generalized Holling type IV functional response and Allee effects in prey. J. Differ. Equ. **309**, 704–740 (2022)
22. Johnson, D.M., Liebhold, A.M., Tobin, P.C., et al.: Allee effects and pulsed invasion by the gypsy moth. Nature **444**(7117), 361–363 (2006)
23. Kent, A., Doncaster, C.P., Sluckin, T.: Consequences for predators of rescue and Allee effects on prey. Ecol. Model. **162**(3), 233–245 (2003)
24. Wang, M.H., Kot, M.: Speeds of invasion in a model with strong or weak Allee effects. Math. Biosci. **171**(1), 83–97 (2001)
25. Dai, G., Tang, M.: Coexistence region and global dynamics of a harvested predator–prey system. SIAM J. Appl. Math. **51**(1), 193–210 (1998)
26. Pauly, D., et al.: Towards sustainability in world fisheries. Nature **418**, 689–695 (2002)
27. González-Olivares, E., Meneses-Alcay, H., et al.: Multiple stability and uniqueness of limit cycle in a Gause-type predator-prey model considering Allee effect on prey. Nonlinear Anal. Real World Appl. **12**, 2931–2942 (2011)
28. Cai, L., Chen, G., Xiao, D.: Multiparametric bifurcations of an epidemiological model with strong Allee effect. J. Math. Biol. **67**(2), 185–215 (2013)
29. Garain, K., Mandal, P.S.: Bubbling and hydra effect in a population system with Allee effect. Ecol. Complex. **47**, 1–14 (2021)
30. Mendez, V., Sans, C., Lopis, I., Campos, D.: Extinction conditions for isolated populations with Allee effect. Math. Biosci. **232**, 78–86 (2011)
31. Rocha, J.L., Fournier-Prunaret, D., Taha, Abdel-Kaddous.: Strong and weak Allee effects and chaotic dynamics in Richards' growths. Discrete Contin. Dyn. Syst. B **18**(9), 2397–2425 (2013)
32. Rocha, J.L., Taha, Abdel-Kaddous., Fournier-Prunaret, D.: Big bang bifurcation in von Bertalanffy's dynamics with strong and weak Allee effects. Nonlinear Dyn. **84**(2), 607–626 (2016)
33. Boukal, D.S., Berec, L.: Single-species models of the Allee effect: extinction boundaries, sex ratios and mate encounters. J. Theor. Biol. **218**, 375–394 (2002)
34. Brassil, C.E.: Mean time to extinction of a metapopulation with an Allee effect. Ecol. Model. **143**, 9–16 (2001)
35. Schreiber, S.J.: Allee effects, extinctions, and chaotic transients in simple population models. Theor. Popul. Biol. **64**(2), 201–209 (2003)
36. Aguirre, P., González-Olivares, E., Sáez, E.: Three limit cycles in a Leslie–Gower predator–prey model with additive Allee effect. SIAM J. Appl. Math. **69**(5), 1244–1262 (2009)
37. Li, C., Rousseau, C.: A system with three limit cycles appearing in a Hopf bifurcation and dying in a homoclinic bifurcation: the cusp of order 4. J. Differ. Equ. **79**, 132–167 (1989)
38. Tang, B., Xiao, Y.N.: Bifurcation analysis of a predator–prey model with anti-predator behaviour. Chaos Solitons Fractals **70**, 58–68 (2015)
39. Huang, J., Gong, Y., Ruan, S.: Bifurcation analysis in a predator–prey model with constant-yield predator harvesting. Discrete Contin. Dyn. Syst. B **18**(8), 2101–2121 (2013)
40. Leard, B., Lewis, C., Rebaza, J.: Dynamics of ratio-dependent predator-prey models with nonconstant harvesting. Discrete Contin. Dyn. Syst. B **1**(2), 303–315 (2008)
41. Yang, Y., Meng, F.W., Xu, Y.C.: Global bifurcation analysis in a predator-prey system with simplified Holling IV functional response and antipredator behavior. Math. Methods Appl. Sci. **1**, 1–19 (2022)
42. Xiao, D., Zhou, Y.: Qualitative analysis of an epidemic model. Can. Appl. Math. Q. **14**(4), 480–484 (2006)
43. Perko, L.: Differential Equations and Dynamical Systems. Springer (2001)
44. Lamontagne, Y., Coutu, C., Rousseau, C.: Bifurcation analysis of a predator-prey system with generalised Holling type III functional response. J. Dyn. Differ. Equ. **20**(3), 535–571 (2008)
45. Shan, C., Zhu, H.: Bifurcations and complex dynamics of an SIR model with the impact of the number of hospital beds. J. Differ. Equ. **257**(5), 1662–1688 (2014)
46. Dumortier, F., Roussarie, R., Sotomayor, J.: Generic 3-parameter families of vector fields on the plane, unfolding a singularity with nilpotent linear part. The cusp case of codimension 3. Ergod. Theory Dyn. Syst. **7**, 375–413 (1987)
47. Chow, S.N., Li, C., Wang, D.: Normal Forms and Bifurcation of Planar Vector Fields. Cambridge University Press, Cambridge (1994)
48. Guckenheimer, J., Holmes, P.: Nonlinear Oscillations, Dynamical Systems and Bifurcations of Vector Fields. Springer-Verlag, New York (1983)

49. Andronov, A.A., Leontovich, E.A., Gordon, I.I., Maier, A.G.: Theory of Bifurcation of Dynamic Systems on a Plane, Israel Program for Science Translation. Wiley, New York (1973)
50. Golubitsky, M., Langford, W.F.: Classification and unfolding of degenerate Hopf bifurcation. J. Differ. Equ. **41**, 375–415 (1981)
51. Zhang, Z., Ding, T., Huang, W., Dong, Z.: Qualitative Theory of Differential Equations. Transl. from the Chinese by Anthony Wing-Kwok Leung (2006)
52. Witte, V.D., Rossa, F.D., Govaerts, W., Kuznetsov, Y.A.: Numerical periodic normalization for codim 2 bifurcations of limit cycles: computational formulas, numerical implementation, and examples. SIAM J. Appl. Dyn. Syst. **12**, 722–788 (2013)
53. Iooss, G.: Global characterization of the normal form for a vector field near a closed orbit. J. Differ. Equ. **76**, 47–76 (1988)
54. Doedel, E.J., Champneys, A.R., Dercole, F., Fairgrieve, T.F., Kuznetsov, Y.A., Oldeman, B., Paffenroth, R., Sandstede, B., Wang, X., Zhang, C.: Auto-07p: continuation and bifurcation software for ordinary differential equations (2007)
55. Govaerts, W., Kuznetsov, Yu.A., Dhooge, A.: Numerical continuation of bifurcations of limit cycles in MATLAB. SIAM J. Sci. Comput. **27**, 231–252 (2005)
56. Xu, Y.C., Wei, L.J., Jiang, X.Y., Zhu, Z.R.: Complex dynamics of a SIRS epidemic model with the influence of hospital bed number. Discrete Contin. Dyn. Syst. B **26**, 1–24 (2021)